

## Responses to Referees

The authors wish to thank both reviewers for their useful suggestions and thoughtful comments. Below are our point-by-point responses to reviewers' comments.

### Referee #1

**Reviewer's comment:** The most important point I would like to make is in regards to the use of hematite particles. Why was Hematite chosen as dust particles for cirrus clouds? Is there prior evidence of its presence in cirrus clouds?

**Authors' response:** We did not select hematite because it is a major atmospheric dust component in cirrus clouds. We chose hematite because it is a good model substance to infer  $n_s$  values over a wide  $T$  and  $RH_{ice}$  range (i.e., page 16500 lines 9-12 and lines 16-21 and Sect. 3.3). The atmospheric relevance was demonstrated by comparing the model hematite results with more relevant desert dust aerosol results (page 16506 lines 20-25).

**Reviewer's comment:** The author refers us to the a paper by *Matsuki et al. (2010)* which examined mineral dust particles from cloud residual and clear sky in Niger. Matsuki et al. shows in Fig 4 in their paper that out of the different types of mineral dust particles that were found in cloud droplets residual, hematite frequency was very small compared to all other mineral dust particles as clay minerals.

**Authors' response:** We cited *Matsuki et al. (2010)* to state that hematite is an example of atmospheric mineral dust particles that can be found as cloud-borne particles, not specifically to infer its presence in cirrus clouds. To clarify our point, we have rephrased "cloud-borne particles" to "cloud-borne particles in shallow stratocumulus clouds" on the page 16506 line 6 in the first manuscript version (now moved to the page 16497 line 21 after "...proxy for atmospheric dust particles).

**Reviewer's comment:** In addition hematite particles are different than most of the atmospheric dust particles (in term of mineralogy and shape), can that also affect their IN ability? Since the atmosphere does not only contain hematite particle but a combination of different dust particles type, why not then combine all dust measurements and try to get an isoline that will represent all of them?

**Authors' response:** In this work, we demonstrated that the formulated hematite  $n_s$ -isolines are reasonably comparable to that of desert dust samples, previously studied in AIDA (i.e., ATD and SD2; *Möhler et al., 2006*), at  $n_s \sim 10^{-11} \text{ m}^{-2}$  (Fig. 3A and associated text on the page 16506 lines 20-25; page 16507 lines 20-22). Nonetheless, we feel it is important to point out and re-emphasize that this work is a conceptual study with laboratory-synthesized hematite particles as a model aerosol for deposition ice nucleation over a wide range of  $T$  and  $RH_{ice}$ . In this study, we did not attempt to conclude how much hematite content contributes to ice formation in cirrus clouds. For clarity, we have added the following sentence on the page 16498 line 3 after "...existing parameterizations.":

"It is important to note that the purpose of the current study is to perform a conceptual study with laboratory-synthesized hematite particles as a model aerosol for deposition ice nucleation, over a wide range of  $T$  and  $RH_{ice}$ , but not to quantify how much hematite content contributes to ice formation in cirrus clouds."

**Reviewer's comment:** Another general comment is that this manuscript will substantially benefit if the author will start the paragraphs with words other than figure or we, in addition there are too many places that are written in first body (e.g. page 16505 lines 4 and 29, page 16506 line 9 etc.).

**Authors' response:** The authors appreciate the prior suggestion by the reviewer on means to improve the overall quality of the paper. As per reviewer's suggestion, we have modified the following sentences (starting with words other than "figure" or "we"):

Sect. 2.2. page 16498 line 23-page 16499 line 3: "For this study, a cooling rate of  $5\text{ }^{\circ}\text{C min}^{-1}$  was typically applied at the beginning. Then, the cooling rate decreased to  $<0.1\text{ }^{\circ}\text{C min}^{-1}$  within 400 s for each pumping expansion experiment, which was mainly due to an increasing heat flux from the chamber walls. Afterwards, an almost constant temperature was maintained by the stirred and well-mixed volume of the cold chamber. During the experiment, the pressure in the vessel decreased from 1000 to 800 mb."

Sect. 2.3. page 16500 line 27: "The mean size and surface area of hematite particles were prescribed with an assumption that..."

Sect. 3.1. page 16504 lines 3-6: "The temporal profiles of deposition nucleation experiments from HALO campaigns, including  $N_{ice}$ , gas  $T$ ,  $\text{RH}_{ice}$  and  $\text{RH}_{water}$  measured by the TDL as well as the polarized light scattering properties in near-backscattering direction measured by SIMONE, are shown in Figure 1."

Sect. 3.1. page 16504 line 20: "The initial  $n_s$ -isoline curves in the  $T$ - $\text{RH}_{ice}$  space are illustrated in Figure 2."

Sect. 3.2. page 16505 lines 27-28: "The  $n_s$ -isolines of hematite particles were compared to previous measurements made using different aerosol species."

Sect. 3.2. page 16506 lines 9-14: "Comparison of the hematite  $n_s$ -isolines to previous deposition freezing observations are shown in Figure 3. More specifically, previous measurements were performed with natural Saharan desert dust (SD2, *Möhler et al.*, 2006), reference Arizona test dust (ATD, *Möhler et al.*, 2006; *Welti et al.*, 2009), volcanic ash (*Steinke et al.*, 2011), soot (*Möhler et al.*, 2005), clay minerals (*Welti et al.*, 2009; *Koehler et al.*, 2010) and organics (*Shilling et al.*, 2006; *Wang and Knopf*, 2011)."

Sect. 3.3. page 16507 lines 24-25: "Next, the ice nucleation efficiency of hematite particles was parameterized over a wide range of  $T$ - $\text{RH}_{ice}$ ."

Sect. 3.4. page 16509 lines 8-9: "The SCAM5 results for monthly mean profiles of the simulated in-cloud  $N_{ice}$  ( $N_i \sim N_{ice}$ ) over the ARM SGP site for five cases are shown in Figure 5."

Sect. 3.4. page 16510 lines 7-8: "The results of the COSMO model for the vertical profiles of  $N_{ice}$  (presumably equivalent to the heterogeneous INP number concentration) are summarized in Figure 7. These results simulate..."

**Reviewer's comment:** A literature overview that shows the actual presence of hematite particles in cirrus clouds is missing. Only in section 3.2 the author mentions the present of hematite particles in the atmosphere but still not in cirrus clouds. It should be mentioned that *Matsuki et al.* (2010) did not mention that the dust particles measurements were taken from cirrus cloud, therefore we need to ask are we sure hematite particles can be found in cirrus clouds?

**Authors' response:** Discussed above.

**Reviewer's comment:** Additional information in the method part is needed. TSI mentioned on the SSPD 3433 web page that it can sufficient deagglomerate most dry particles in the range from 0.5 to 50  $\mu\text{m}$ , in the paper the authors mention that they size selected 200nm, which is below the threshold of this equipment.

**Authors' response:** The previous AIDA study (Fig. 2 of *Skrotzki et al.*, 2013) demonstrated the application of a SSPD for dry-dispersion of quasi-monodisperse (200 nm mode diameter) hematite into the AIDA vessel.

Page 16498 lines 16-17 now reads:

“A Small-Scale Powder Disperser (SSPD, TSI, Model 3433) was used to dry-disperse the quasi-monodispersed hematite particles into the AIDA vessel as demonstrated in *Skrotzki et al.* (2013).”

Reference:

Skrotzki, J., Connolly, P., Schnaiter, M., Saathoff, H., Möhler, O., Wagner, R., Niemand, M., Ebert, V., and Leisner, T.: The accommodation coefficient of water molecules on ice – cirrus cloud studies at the AIDA simulation chamber, *Atmos. Chem. Phys.*, 13, 4451-4466, doi:10.5194/acp-13-4451-2013, 2013.

**Reviewer's comment:** In addition, did the author verify that the size that were selected by the DMA were similar to the size distribution that came out of the DMA?

**Authors' response:** DMA was not employed in our study. As described in lines 6-12 of the page 16498, we used laboratory-synthesized hematite particles that had been formed as a powder of equally sized hematite particles (~200 nm, 500 nm, 1000 nm area equivalent diameter; *Skrotzki et al.*, 2013; *Hiranuma et al.*, 2014). Hence, no additional size-segregation was necessary.

Reference:

Hiranuma, N., Hoffmann, N., Kiselev, A., Dreyer, A., Zhang, K., Kulkarni, G., Koop, T., and Möhler, O.: Influence of surface morphology on the immersion mode ice nucleation efficiency of hematite particles, *Atmos. Chem. Phys.*, 14, 2315–2324, doi:10.5194/acp-14-2315-2014, 2014.

**Reviewer's comment:** Section 2.3 page 16500 line 27 to page 16501 line 3. Was a 1000nm surface area used for all three selected sizes, please clarify?

**Authors' response:** We chose only 1000 nm diameter as a simulated hematite size for our COSMO and SCAM5 modeling studies. Our choice of 1000 nm diameter and surface area is reasonable and representative for ice nucleation efficiency (inferred by  $n_s$ ) of three different sizes of hematite particles studied at AIDA (page 16503 lines 18-25; i.e., different sizes of hematite particles were used to characterize ice nucleation efficiency,  $n_s$ , at a wide temperature range).

**Reviewer's comment:** The value of 1000nm that were taken from *Hiranuma et al.* (2014) does not represent size selected measurement but values from looking on the entire distribution, does the authors expect it to be the same value?

**Authors' response:** We use the term ‘quasi-monodisperse’ because of the presence of minor fraction of smaller agglomerates/fragments (Fig. 2 in *Skrotzki et al.*, 2013; Fig. 1 in *Hiranuma et al.*, 2014) within the sample, but this minor fraction have minimum influence on the surface-scaled  $n_s$  parameterization presented in the current work.

The geometric standard deviation ( $\sigma_g$ ) from *Hiranuma et al.* (2014) is correctly 1.05. What we have reported (0.097) is “width of the distribution” ( $= 2.303 \cdot 2 \log \sigma_g$ ; *Huffman et al.*, 2010). Our COSMO and SCAM5 modeling studies were performed based on either assuming monodisperse size distribution of 1000 nm or mode diameter of 1000 nm with  $\sigma_g = 1.05$ . After all, the impact of introducing

such distribution on the simulation results was small as presented in the manuscript (page 16509 line 28- page 16510 line 1).

For consistency, we have replaced “( $\sigma = 0.097$ )” with “( $\sigma_g = 1.05$ )” on page 16501 line 2.

Reference:

Huffman, J.A., Treutlein, B., and Pöschl, U.: Fluorescent biological aerosol particle concentrations and size distributions measured with an Ultraviolet Aerodynamic Particle Sizer (UV-APS) in Central Europe, *Atmos. Chem. Phys.*, 10, 3215-3233, doi:10.5194/acp-10-3215-2010, 2010 (the supplemental Online Material is available at: <http://www.atmos-chem-phys.net/10/3215/2010/acp-10-3215-2010-supplement.pdf>).

**Reviewer’s comment:** Page 16501 line 13 The author mentioned that for  $T > -36$  the parameterization from M92 was used in the model, however it is known (and also mentioned on the page 16496 line 21) that M92 parameterization is relevant for  $-7 > T > -23$ , therefore I am not sure if the model can represent well the creation of ice for temperature between  $-23 < T < -36$ .

**Authors’ response:** We agree with the reviewer that the M92 parameterization, which was developed based on the INP concentrations from CFDC observations in mid-latitudes, is strictly valid only in the temperature and supersaturation range of the measurements, i.e., between  $-7$  and  $-20^\circ\text{C}$  and 2 and 25% ice supersaturation. However, it has been extrapolated beyond this range in numerous previous model implementations (e.g., *Morrison et al.*, 2003; *Seifert and Beheng*, 2006), because some information is needed in the whole temperature range above homogeneous freezing conditions. Here, we implemented the M92 parameterization, for  $T > -36^\circ\text{C}$ , where hematite particles are not ice active, simply to ensure a reasonable spatio-temporal distribution of total water content (among water vapor, liquid and ice phase cloud particles) and to avoid unrealistic conditions (e.g., high supersaturations) in the lower troposphere in our model runs. Further, Figure 2 in *Seifert et al.* (2012) show the evidence that the deviation between the Phillips parameterization (*Phillips et al.*, 2008) and the M92 parameterization can result in about an order of magnitude INP concentration mainly due to ‘aerosol assumption’ (i.e., number concentration). For these reasons, and given the inherent uncertainty of an aerosol-independent approach, we believe that the use of the M92 parameterization for  $T > -36^\circ\text{C}$  in our conceptual modeling study is appropriate and reasonable.

References:

Morrison, H., Shupe, M. D., and Curry, J. A.: Modeling clouds observed at SHEBA using a bulk microphysics parameterization implemented into a single-column model, *J. Geophys. Res.*, 108, doi:10.1029/2002JD002229, 2003.

Seifert, A., Köhler, C., and Beheng, K. D.: Aerosol-cloud-precipitation effects over Germany as simulated by a convective-scale numerical weather prediction model, *Atmos. Chem. Phys.*, 12, 709–725, doi:10.5194/acp-12-709-2012, 2012.

Seifert, A. and Beheng, K.D.: A two-moment cloud microphysics parameterization for mixed-phase clouds. Part I: Model description, *Meteorol. Atmos. Phys.*, 92, 45–66, doi:10.1007/s00703-005-0112-4, 2006.

Phillips, V.T.J., DeMott, P.J., and Andronache, C.: An empirical parameterization of heterogeneous ice nucleation for multiple chemical species of aerosol, *J. Atmos. Sci.*, 65, 2757–2783, doi:<http://dx.doi.org/10.1175/2007JAS2546.1>, 2008.

**Reviewer’s comment:** Page 16506 lines 4-8 I think that this part should also be mentioned in the introduction part.

**Authors’ response:** The referee makes a good point. We have updated and moved the following sentence on the page 16497 line 21 after “...proxy for atmospheric dust particles”:

“Hematite is used as an example of atmospheric mineral dust particles, which can also be found in the form of cloud-borne particles in shallow stratocumulus clouds (*Matsuki et al.*, 2010). Natural hematite often exists in supermicron-sized silt particles and accounts for a few percent of the total dust particle mass (*Claquin et al.*, 1999).”

**Reviewer’s comment:** Page 16507 lines 14-22 Can the author say something about some of the points on figure 3 that does not match the  $n_s$  isoline, spatially those measured by AIDA.

**Authors’ response:** The reviewer is right. It may be indicative of isolines to be also as a function of composition. The authors, however, point out that the previous AIDA results for desert dust are in good agreement with the new  $n_s$  isolines, at least within an order of magnitude, and their agreement also supports the general trend of the isolines. There is one outlier for SD2 at about  $-50^\circ\text{C}$ . The reason for which is not known. Furthermore, the soot data show a somewhat less steep increase to lower temperatures. But, it confirms the general trend of isolines for deposition nucleation. These premises must be further examined in comparing to atmospherically relevant substrates and their ice nucleation activities in controlled laboratory settings.

**Reviewer’s comment:** Page 16508 lines 3 I think that the part of supplement material 3 should be part of the paper, since all the measurements represent measurement below water saturation the reader should see in detail how that isonline above water saturation were calculated.

**Authors’ response:** The authors prefer to keep it in the supplement. To address the reviewer’s concern, we now rephrased the sentences in the page16508 lines 1-3 as:

Original: “The lower bound of  $n_s$  value ( $10^6 \text{ m}^{-2}$ ) was set based on the minimum  $n_s$  observed during AIDA expansions. The method used to constrain the  $n_s$ -isolines above 100%  $\text{RH}_{\text{ice}}$  as discussed in the supplemental material (Fig. S3).”

→

Modified: “The lower bound of  $n_s$  value ( $10^6 \text{ m}^{-2}$ ) was set based on the minimum  $n_s$  observed during AIDA expansions. Since the certain regions of  $n_s$ -isolines (i.e.,  $n_s < 7.5 \times 10^{10} \text{ m}^{-2}$ ; blue lines in Fig. 2) can submerge below ice saturation, the correction was applied to shift them and maintain all isolines above 100%  $\text{RH}_{\text{ice}}$ . The procedure to constrain  $n_s$  to  $>100\% \text{ RH}_{\text{ice}}$  is described in the supplement (Fig. S3).”

**Reviewer’s comment:** Page 16508 lines 12-17 (regarding Figure 4b) Why using a third degree polynomial if it does not represent the experimental work?

**Authors’ response:** In later sections (i.e., Simulation A vs. Simulation B in Figs. 5, 6 and 7 in Sect. 3.4), we demonstrate that the third degree polynomial fit parameterization yield similar simulation results (with respect to yielded ice crystal concentration) compared to the interpolated parameterization. We intended to introduce this fit owing to its model friendly aspect.

**Reviewer’s comment:** Page 16509 first paragraph The whole section is not clear. It is not clear, which figure represent figure 4b? Some of the sentence needs clarification as lines 14-20. There is hardly reference to figure 6.

**Authors’ response:** To clarify our study cases, we have modified and updated the texts in the following sections:

Page 16509 lines 9-13:

Original: “These include the pure homogeneous ice nucleation case (Simulation A), three cases with contributions from both the homogeneous and heterogeneous ice nucleation (hereafter combined case) described in Fig. 4 (Simulations B, C and D) and the simulation of the different lower boundaries of  $RH_{ice}$  ( $RH_i^*$ , Simulation D).”

→

Modified: “These include (Case 1) the pure homogeneous ice nucleation case, (Case 2-4) cases with contributions from both homogeneous and heterogeneous ice nucleation (hereinafter referred to as the combined case) described in Fig. 4a-c (corresponding to Simulations A, B and C) and (Case 5) the simulation of the different lower boundaries of  $RH_{ice}$  ( $RH_i^*$ , Simulation D).”

Page 16509 lines 18-20:

Original: “The differences between the four parameterizations used in this study are small for both the combined cases and the pure heterogeneous cases.”

→

Modified: “The differences between the three parameterizations derived from AIDA measurements, corresponding to Simulations A, B and D, are small for both the combined case and the pure heterogeneous ice nucleation case as presented in Fig. 6.”

Page 16509 line 25:

Original: “The three parameterizations have largest differences...”

→

Modified: “The three parameterizations (i.e., Simulations A, B and D) have largest differences...”

**Reviewer’s comment:** Discussions: The first paragraph is not so clear, the SCF was mentioned only briefly in section 3.2. I recommend the authors to rewriting this paragraph again.

**Authors’ response:** We now updated the first paragraph on the page 16511:

“As described in the previous section (Sect. 3.1), deposition mode freezing cannot solely explain the  $n_s$ -isoline observation below water saturation ( $-50\text{ °C} < T < -36\text{ °C}$  in Fig. 2). Although we presumed that SCF acts as a subset of immersion freezing and plays an important role in this region, further insight and evidence of SCF beyond cloud simulation chamber observations are required to correctly understand the contributions of both homogeneous and heterogeneous nucleation. High-resolution microscopic techniques with an integrated continuous cooling setup are needed to visualize the freezing process of a single particle and to fully understand the complex freezing processes involved in SCF on particle surfaces.”

We feel the definition of SCF given in Sect. 3.1 (page 16505 lines 14-25) is sufficient and no repetitive discussion is necessary.

**Reviewer’s comment:** Page 16511 lines 21-23 Not all the points on figure 3 match the hematite particles therefore I do not think it is correct to assume that all dust will behave in the same way is hematite particles.

**Authors’ response:** To address the referee’s concern, we now rephrased the related section.

Page 16511 lines 21-23:

Original: In fact, comparison between our AIDA  $n_s$ -based parameterization with hematite particles and *Möhler et al. (2006)* with ATD and SD2 (Fig. 3a) provides indication on the validity of the assumption to treat all dust as hematite in deposition mode.”

→

Modified: “In fact, comparison between our AIDA  $n_s$ -based parameterization with hematite particles and *Möhler et al. (2006)* with ATD and SD2 (Fig. 3a) suggests that hematite has similar ice nucleation efficiency, inferred by  $n_s$ , as dust. The comparison between the observed profile of ice crystal number concentrations and the simulated ones (Figs. 5 and 6) also suggests the validity of the new parameterizations. These premises must be further examined in comparing to atmospherically relevant substrates (fresh and aged ones) and their ice nucleation activities in laboratory settings. In situ INP measurements, such as the number concentration and the types of INPs, at the upper troposphere can also help to constrain the parameterizations.”

**Reviewer’s comment:** Table 1:

Organize the table in a way that will be easier on the reader, for example based on  $T$  from warm to cold  $T$  or particle size.

**Authors’ response:** Table 1 is now organized based on T(Evaluated  $n_s$ ) - from low to high T(Evaluated  $n_s$ ).

Table 1. Summary of aerosol measurements and AIDA ice nucleation experiments. All HALO experiments are from *Skrotzki et al. (2013)*.

Experiment ID	Aerosol Measurements			Ice Nucleation Measurements				
	Hematite Diameter, nm	Total Number Conc., cm <sup>-3</sup>	Total Surface Conc., μm <sup>2</sup> cm <sup>-3</sup>	Examined T Range, °C	Examined RH <sub>ice</sub> Range, %	Evaluated $n_s$ , m <sup>-2</sup>	T(Evaluated $n_s$ ), °C	RH <sub>ice</sub> (Evaluated $n_s$ ), %
HALO05_24	200	115.0	14.4	-76.1 to -81.9	100.6 to 164.8	10 <sup>11</sup>	-78.2	136.4
HALO04_09	500	112.5	26.9	-75.8 to -80.1	100.3 to 149.8	10 <sup>11</sup>	-77.5	128.3
HALO04_05	500	142.2	30.9	-61.8 to -65.5	100.2 to 135.6	10 <sup>11</sup>	-62.6	111.1
HALO05_18	200	161.9	21.8	-60.3 to -65.2	100.1 to 124.5	10 <sup>11</sup>	-60.8	106.0
HALO06_22	200	145.7	19.2	-50.2 to -53.9	100.3 to 123.4	10 <sup>11</sup>	-50.7	106.7
HALO06_21	200	245.0	32.9	-50.3 to -53.8	100.4 to 115.8	10 <sup>11</sup>	-50.5	102.2
INUIT01_26	1000	342.1	749.0	-41.0 to -47.1	100.2 to 103.9	10 <sup>10</sup>	-41.2	102.2
HALO06_20	200	168.7	22.4	-39.8 to -44.4	100.4 to 128.8	10 <sup>10</sup>	-40.7	111.3
HALO06_19	200	283.0	42.9	-39.7 to -44.5	100.2 to 121.6	10 <sup>10</sup>	-40.6	109.2
INUIT04_08	1000	193.0	647.0	-39.3 to -45.4	100.0 to 113.2	10 <sup>10</sup>	-40.4	110.1
INUIT04_10	1000	161.7	546.6	-37.5 to -43.7	100.0 to 124.1	10 <sup>10</sup>	-40.1	123.3
INUIT01_30	1000	414.5	889.7	-34.6 to -42.0	100.2 to 127.1	2.5 x 10 <sup>8</sup>	-37.0	122.8

**Reviewer’s comment:** Please add to the table a column that will give information on which of experiments were taken from Skrotzki et al. (2013) and which one from Hiranuma et al. (2014) etc.

**Authors' response:** We have updated the table text as “Table 1. Summary of aerosol measurements and AIDA ice nucleation experiments. All HALO experiments are from *Skrotzki et al. (2013)*.”. Further information is given in text on the page 16503 lines 13-17.

**Reviewer's comment:** No information regarding how the evaluated  $n_s$  values of  $T$  and  $RH$  is mentioned in the text, why and how these value were chosen?

**Authors' response:** We thank the reviewer for pointing out this error. We have added information regarding “evaluated  $n_s$ ,  $T$  and  $RH_{ice}$ ”, which were used to verify size-independency of the  $n_s$  values (page 16503 lines 18-25), in the following sections:

Page 16503 line 21

Original: "the  $n_s$  values"

→

Modified: "the evaluated  $n_s$  values"

Page 16503 lines 22-23

Original: “(i.e., INUIT04\_08, 1000 nm, HALO06\_19,200 nm, and HALO06\_20, 200 nm)”

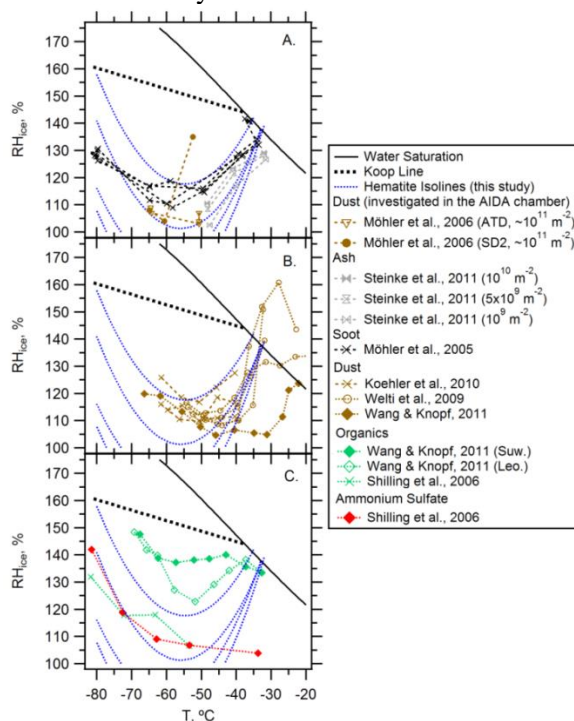
→

Modified: “(see corresponding  $RH_{ice}$  and  $T$  at Evaluated  $n_s$  in Table 1 for INUIT04\_08, 1000 nm, HALO06\_19, 200 nm, and HALO06\_20, 200 nm)”

**Reviewer's comment:** Figure 2 and 3

It will be better to increase the figures size on the expend of the legend which take too much space of the figure, which does not allow to see all the values.

**Authors' response:** Modified with smaller symbols.

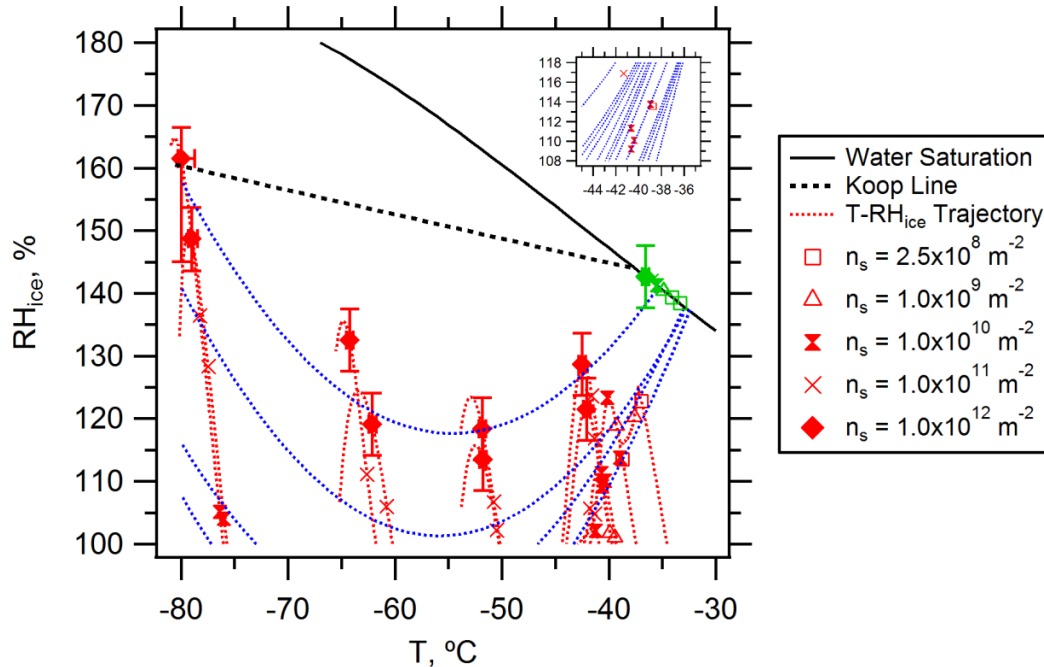




**Reviewer’s comment:** Figure 2

It is very hard to distinguish between the different values; it might be the red color, especially around -40°C where the points are overlapping one another. Please mark them in a different marker or color. Please also mark in a different color the immersion freezing measurement so it will be easy to identify them from the one from this work (mentioned also on the page 16504 lines 23).

**Authors’ response:** We modified Figure 2 with smaller symbols as well as its caption as:



Original caption: “...The data on the water saturation line represents the previously reported results of immersion freezing (*Hiranuma et al.*, 2014).”

→

Modified: “...The data indicated by green color on the water saturation line represent the previously reported results of immersion freezing (*Hiranuma et al.*, 2014).”

**Reviewer’s comment:** Figure 5 and 6

It is very hard to distinguish between some of the lines. Perhaps using another color indicator or showing only pressure of 0-600 will highlight the differences. An addition line which will represent observation will be a nice addition for this plot, something that will represent the observation to show how the new parameterization is compared to it.

**Authors’ response:** This is a good suggestion. We added the observed profiles of ice crystal number concentrations in the figure. The observational data were collected over the SGP site on eight days of April 2010 during the Small PARTICles In Cirrus (SPARTICUS) campaign (*Zhang et al.*, 2013). See the figure 5&6 captions for details. Please note that for the aircraft measurements, we only consider samples when ice crystal number is above the detection limit (*Zhang et al.*, 2013). Accordingly, for modeled profiles we replaced the grid-box mean values with the in-cloud values.

Reference:

Zhang, K., Liu, X., Wang, M., Comstock, J. M., Mitchell, D. L., Mishra, S., and Mace, G. G.: Evaluating and constraining ice cloud parameterizations in CAM5 using aircraft measurements from the SPARTICUS campaign, *Atmos. Chem. Phys.*, 13, 4963-4982, doi:10.5194/acp-13-4963-2013, 2013.

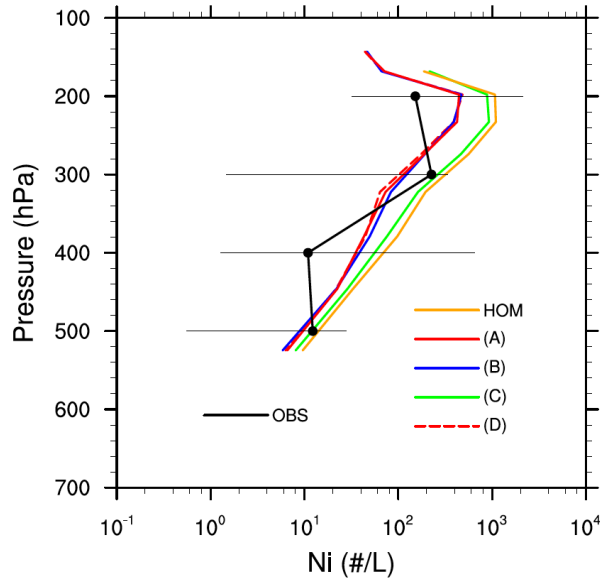


**Figure 5.** Monthly mean profiles of the simulated in-cloud ice crystal number concentrations ( $N_i \sim N_{ice}$ ) over the ARM SGP site. The four cases shown in the figure include the pure homogeneous ice nucleation case (HOM) and four combined (heterogeneous + homogeneous) ice nucleation cases: (A) AIDA Interp. + Homogeneous; (B) AIDA Fit + Homogeneous; (C) P13 + Homogeneous; and (D) AIDA Interp. ( $RH_i^* = 105\%$ ) + Homogeneous. Black dots show the observed mean profile of  $N_i$ . Left and right ends of the horizontal bars indicate the 10<sup>th</sup> and 90<sup>th</sup> percentiles of the observed  $N_i$  values at each pressure level.

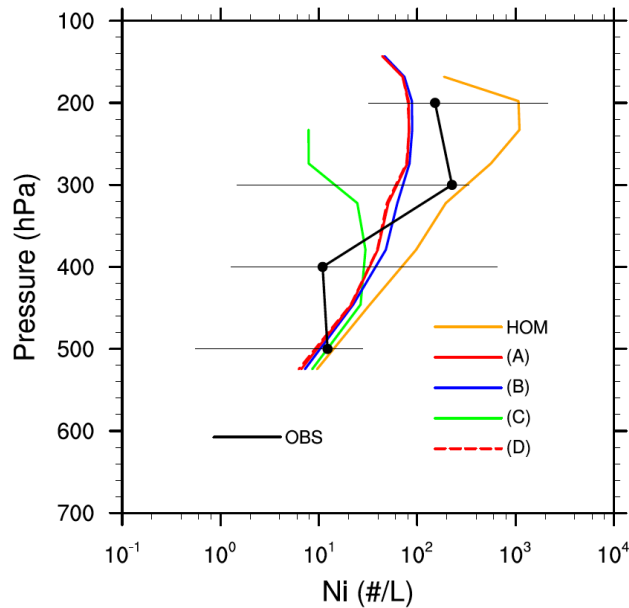


**Figure 6.** Monthly mean profiles of the simulated in-cloud ice crystal number concentrations ( $N_i \sim N_{ice}$ ) over the ARM SGP site. The four cases shown in the figure include the pure homogeneous ice nucleation case (HOM) and four pure heterogeneous ice nucleation cases: (A) AIDA Interp.; (B) AIDA Fit; (C) P13; and (D) AIDA Interp. ( $RH_i^* = 105\%$ ). Black dots show the observed mean profile of  $N_i$ . Left and right ends of the horizontal bars indicate the 10<sup>th</sup> and 90<sup>th</sup> percentiles of the observed  $N_i$  values at each pressure level.

We added the following sentence on the page 16509 line 13 after "... Simulation D).":

"In addition, the observed profile of ice crystal number concentrations is also shown in comparison to the simulations in Fig. 5. The observational data were collected over the SGP site on eight days of April 2010 during the Small PARTICles In Cirrus (SPARTICUS) campaign (Zhang *et al.*, 2013)."

We added the following sentence on the page 16509 line 18 after "... heterogeneous nucleation.":

"The observed mean profile of in-cloud ice crystal number concentrations is in agreement with the simulated ones."

We also modified the sentences on the page 16511 lines 20-23:

Original: In fact, comparison between our AIDA  $n_s$ -based parameterization with hematite particles and *Möhler et al.* (2006) with ATD and SD2 (Fig. 3a) provides indication on the validity of the assumption to treat all dust as hematite in deposition mode."

→

Modified: "In fact, comparison between our AIDA  $n_s$ -based parameterization with hematite particles and *Möhler et al.* (2006) with ATD and SD2 (Fig. 3a) suggests that hematite has similar ice nucleation efficiency, inferred by  $n_s$ , as dust. The comparison between the observed profile of ice crystal number concentrations and the simulated ones (Figs. 5 and 6) also suggests the validity of the new parameterizations. These premises must be further examined in comparing to atmospherically relevant substrates (fresh and aged ones) and their ice nucleation activities in laboratory settings. In situ INP measurements, such as the number concentration and the types of INPs, at the upper troposphere can also help to constrain the parameterizations."

**Reviewer's comment:** Consider changing figure 5 and 6 to one figure as 5a and b, it will be easier for the reader to understand the comparison of the two.

**Authors' response:** We use another alphabetical sub-category (Simulations A-D), and we feel introducing another one will be confusing. We now modified the text and introduced Figure 6 explicitly at the reviewer's prior suggestion. So we would like to keep figure numbers as is.

**Additional revision:** In addition to addressing the reviewer's comments, other editorial corrections (major and non-miscellaneous ones) were made as below.

Since a temperature is a numerical measure, we would like to replace "warm or cold" with "high or low":  
page 16494 line 14, page 16494 line 16, page 16494 line 21, page 16500 line 21, page 16504 line 16,  
page 16511 line 13.

Abstract

Page 16494 lines 4-5: "critical in order to" → "important to"

Page 16494 line 8: "water saturated conditions that were realized" → "water subsaturated conditions. These conditions were achieved"

Introduction

Page 16495 line 2: "constitute" → now rephrased to "represent a"

Page 16495 lines 15-19: now reads, “Briefly, deposition mode induces ice formation when water vapor is directly deposited onto the INP, immersion and condensation freezing can induce ice formation when freezing is initiated by the INP immersed within the supercooled droplet or solution droplet, and contact freezing can initiate at the moment when an INP comes into contact with a supercooled droplet.”

Page 16495 line 21: “is accounted for by” → now reads, “results from”

Page 16495 lines 22-24: “However, representativeness of freezing mechanisms in cirrus clouds is still ambiguous (e.g., *Sassen and Khvorostyanov*, 2008).” → now reads, “However, freezing mechanisms in cirrus clouds are still uncertain (e.g., *Sassen and Khvorostyanov*, 2008).”

Page 16496 line 19: “descriptions such as *Meyers et al.* (1992, henceforth M92)” → now reads, “descriptions given in *Meyers et al.* (1992, hereinafter referred to as M92)”

Page 16497 lines 4-6: now reads, “They showed that the heterogeneous INP number concentration obtained from a CNT-based parameterization is typically higher by several factors than that of Phillips’s parameterization under identical test conditions”

Page 16497 lines 19-20: “Herein, as part of the Ice Nucleation research UnIT (so called INUIT), we conducted a comprehensive investigations on examining the” → now reads, “Within the framework of Ice Nucleation research UnIT (INUIT), we comprehensively investigated”

Page 16497 lines 26-28: “Applications of the fitted  $n_s$  parameterization derived from these measurements to atmospheric modeling simulations were also performed.” → now reads, “In addition to developing the new dust parameterizations from these AIDA measurements (Sects. 3.1-3.3), the fitted  $n_s$  parameterization was also applied to atmospheric modeling simulations (Sect. 3.4).”

## Method

Page 16498 lines 7-10: “well defined surface area, and are therefore good to investigate and relate  $T\text{-RH}_{\text{ice}}$  dependent ice nucleation efficiency to surface area (*Hiranuma et al.*, 2014).” → now reads, “well-defined surface area. Hence, they are suited well for investigating  $T\text{-RH}_{\text{ice}}$ -dependent ice nucleation efficiency and relating it to the surface area (*Hiranuma et al.*, 2014).”

Page 16500 line 19: “complementally covering” → now reads, “that complement each other and cover”

Page 16501 lines 12-14: “was used to simulate ice formation of background particles at  $T > -36^\circ\text{C}$ . In specific, the aerosol-independent M92 scheme was used in this study. A combination of these parameterizations was advantageous...” → now reads, “was used to simulate ice formation of background particles at  $T > -36^\circ\text{C}$ , namely, the aerosol-independent M92 scheme. These parameterizations were combined...”

Page 16501 line 18: “To better understand how the AIDA  $n_s$ -based parameterization compares to” → now reads, “To better understand to what an extent the AIDA  $n_s$ -based parameterization differs from”

Page 16502 lines 4-8: now reads, “The single column model resembles a single column of a GCM and can be derived from observations or model output. The complex feedbacks between the simulated column and other columns due to large-scale dynamics, except cloud detrainment from shallow and deep convection, are not considered. Therefore, the single column model is an ideal tool for testing ice cloud parameterizations.”

Page 16502 lines 20-21: “More specifically, COSMO is the high resolution limited-area model, which allows an assessment of clouds” → now reads, “COSMO is the high-resolution limited-area model to assess clouds”

## Results

Page 16503 lines 13-14: “In the present study we also used the AIDA results reported in *Skrotzki et al.* (2013) and reconciled to  $n_s$  values” → now reads, “In addition, we used the AIDA results reported by *Skrotzki et al.* (2013) and reconciled them with the  $n_s$  values”

Page 16503 lines 25-26: “Further, an advantage of using 1000 nm diameter hematite particles was that, being of , comparatively larger surface area,” → now reads, “The advantage of using 1000 nm diameter hematite particles was that, due to their comparatively larger surface area,”

Page 16505 line 16: “Supportively,” → now reads, “To support this,”

Page 16505 line 21: “SCF may have plausible relevance” → now reads, “SCF may be of relevance”

Page 16507 lines 14-16: now reads, “As seen in Figure 3, the results from previous studies suggest the necessity of increasing  $RH_{ice}$  to maintain a constant  $n_s$  value below  $T \sim -55^\circ\text{C}$ . They also indicate that nucleation may be triggered by SCF...”

Page 16508 lines 7-8: “are necessary in order to” → now reads, “are required to”

Page 16508 lines 17-20: now reads, “The third approach (Fig. 4c) consisted in applying the equivalent  $n_s$  for deposition nucleation of hematite particles parameterized using the method introduced by *Phillips et al.* (2008 and 2013). In detail, we characterized the nucleation activity...”

Page 16509 lines 13-14: “We observe that ice crystal formation from” → now reads, “The results of our simulations suggests that ice crystal formation due to”

Page 16509 line 24: “balances” → now rephrased to “compensates”

Page 16510 line 21: “This enables us to estimate” → “This segregation allows for an estimation of”

## Discussion

Page 16511 line 14: “and deserves more attention.” → now reads, “, and this highlights the need for further investigation.”

Page 16511 line 24 – Page 16512 line 2: now reads, “Finally, to further develop more atmospherically relevant parameterizations other than the fit-based parameterization with artificial test aerosol, the relationship between  $1/T$  and  $\ln S_{ice}$  for a constant nucleation rate or  $n_s$  based on the CNT can be analyzed (i.e., Eqns. A10-A11 in *Hoose and Möhler, 2012*). In this way, the composition specific  $n_s(T-S_{ice})$  values, where the transition from SCF to deposition nucleation (or vice versa) occurs, may be better defined and can be then be used as an inexpensive model friendly parameterization.”

## Conclusion

Page 16512 lines 21-23: “Elaborating observed suppression of SCF near water saturation and enlightening the physical processes on observed transitions in nucleation modes for various types of atmospheric particles are important as future works.” → now reads, “The observed active SCF near water saturation and physical processes at the transitions of nucleation modes still remain to be studied in detail for various types of atmospheric particles.”

Page 16513 lines 1-5: now reads, “Our new parameterization revealed a minimum deviation of  $N_{ice}$  values estimated by SCAM5 at minimum  $RH_{ice}$  values for ice formation (100 or 105%) compared to COSMO. This deviation suggests different sensitivities of the model to the lower bound of the  $RH_{ice}$  value owing to the presence of the model-resolved supersaturation...”

Page 16513 line 7: “suppression in ice nucleation” → now rephrased to “more ice nucleation”

## References

Pages 16514-16519: All available doi numbers are now added in references.

Page 16517: Mishra et al., which is a study on optical properties, has been excluded.

## Referee #2

**Reviewer's comment:** 1) Justification for using hematite to represent "atmospheric dust" at the start of the paper, or stating this as a point of evaluation in this manuscript.

**Authors' response:** We have updated the last paragraph of the introduction section with some more clarification on why we selected hematite particles as a test substrate as well as a proxy of atmospheric dust in this study.

We chose hematite because it is a good model substance to infer  $n_s$  values over a wide  $T$  and  $\text{RH}_{\text{ice}}$  range (i.e., page 16500 lines 9-12 and lines 16-21 and Sect. 3.3). The atmospheric relevance was demonstrated by comparing the model hematite results with more relevant desert dust aerosol results (page 16506 lines 20-25).

In this work, we demonstrated that the formulated hematite  $n_s$ -isolines are reasonably comparable to that of desert dust samples, previously studied in AIDA (i.e., ATD and SD2; Möhler *et al.*, 2006), at  $n_s \sim 10^{-11} \text{ m}^{-2}$  (Fig. 3A and associated text on the page 16506 lines 20-25; page 16507 lines 20-22). Nonetheless, we feel it is important to point out and re-emphasize that this work is a conceptual study with laboratory-synthesized hematite particles as a model aerosol for deposition ice nucleation over a wide range of  $T$  and  $\text{RH}_{\text{ice}}$ . In this study, we did not attempt to conclude how much hematite content contributes to ice formation in cirrus clouds. For clarity, we have added the following sentence on the page 16498 line 3 after "...existing parameterizations.":

"It is important to note that the purpose of the current study is to perform a conceptual study with laboratory-synthesized hematite particles as a model aerosol for deposition ice nucleation, over a wide range of  $T$  and  $\text{RH}_{\text{ice}}$ , but not to quantify how much hematite content contributes to ice formation in cirrus clouds."

**Reviewer's comment:** 2) Recognizing the fact that P13 is at least inclusive of some atmospheric INP data, so the mystery of it not agreeing with lab data below  $-40^\circ\text{C}$  is neither a new discovery, nor is it explained by new data presented herein. As an explanation of lower temperature discrepancies with laboratory dust data, P13 offered that coatings are common and may limit deposition nucleation. This may not be the full reason, but this paper needs to better explain or speculate as to why the modeling community should use the new parameterization in preference to P13.

**Authors' response:** The referee makes a good point in stating the fact that we are not working on the premise that there is one true dust-derived  $n_s(T, S_i)$  and thus we cannot conclusively say which parameterization does better job for predicting/estimating dust-derived INPs. To address referee's concern, we modified the relevant texts and also soften the tense of P13 vs. our new parameterization in the following sections:

Page 16510 lines 24-27:

Original: "Our result shows less ice crystal formation with P13 compared to the AIDA  $n_s$ -isoline-based parameterization. The observed discrepancy between the new parameterization and P13 may largely reflect the difference in parameterization based on lab- or field data. Furthermore, strong supersaturation dependence of  $n_s$  at cold  $T$  was not well constrained by P13, presumably due to a limited amount of data."  
→

Modified: "Our results show diversity between P13 and the AIDA  $n_s$ -isoline-based parameterization. Ice crystal formation was less for P13 and more for the new parameterization. A possible explanation for the observed deviation may be due to the difference in parameterization based on lab- or field data. For

instance, atmospheric aging and processing (i.e., surface coating and associated heterogeneous surface reactions) may have altered ice-nucleating propensity and limited deposition nucleation of dust-derived INPs in the P13 parameterization for the field data-derived parameterization as discussed in *Phillips et al.* (2008).”

Page 16511 lines 14-23:

Original: “Substantial differences between the empirical approach of P13 and our parameterization developed in this study are presumably attributed to the difference in lab- or field data, highlighting the need for further characterizations of atmospherically relevant substrates and their ice nucleation activities in laboratory settings. Nevertheless, *Niemand et al.* (2012) demonstrated that different dusts exhibit similar  $n_s$  in immersion mode freezing and perhaps such a similarity remains true for deposition mode ice nucleation. In fact, comparison between our AIDA  $n_s$ -based parameterization with hematite particles and *Möhler et al.* (2006) with ATD and SD2 (Fig. 3a) provides indication on the validity of the assumption to treat all dust as hematite in deposition mode.”

→

Modified: “However, it should be noted that there is some evidence for the atmospheric relevance and applicability of the new parameterization. First of all we demonstrated that the new  $n_s$  parameterization based on the experiments with hematite particles agrees well with previous literature results for mineral dust aerosol (e.g., *Möhler et al.*, 2006; *Welti et al.*, 2009; *Köhler et al.*, 2010). Second, *Niemand et al.* (2012) demonstrated that different dusts exhibit similar  $n_s$  in immersion mode freezing and perhaps such a similarity remains true for the deposition mode ice nucleation of desert dusts. Lastly, the comparison between the observed profile of ice crystal number concentrations and the simulated ones (Figs. 5 and 6) also suggests the validity of the new parameterization. These premises must be further examined in comparing to atmospherically relevant substrates (fresh and aged ones) and their ice nucleation activities in laboratory settings. In situ INP measurements, such as the number concentration and the types of INPs, at the upper troposphere can also help to constrain the parameterization.”

Page 16509 lines 3-6:

Original: “To conclude, the discrepancy between a new parameterization and P13 is substantially large, and the consequence of this discrepancy towards cloud properties is demonstrated in the following section.”

→

Modified: “AIDA  $n_s$ -isoline-based parameterization suggests strong supersaturation dependence of  $n_s$  at low  $T$ . Observed diversity between a new parameterization (Figs. 4a and 4b) and P13 (Fig. 4c) may result in different ice crystal forming propensities and may predict different cloud properties. The potential consequence of observed diversity is demonstrated using conceptual models and discussed in the following section.”

In addition, we also moved the following discussion of upper and lower  $T$  boundary (originally page 16508 line 24- page 16509 line 3) and inserted to the page 16508 line 17, after “... shown in Fig. 4b.” since these boundaries are more relevant to  $n_s$  fit presented in Fig. 4b:

“Note that the upper temperature boundary of  $-36$  °C was assigned as the interface between immersion mode- and deposition mode ice nucleation (*Hiranuma et al.*, 2014), and the lower boundary of  $-78$  °C is the limit introduced by interpolating the hematite-isoline curves.”

**Reviewer’s comment:** 3) Relatedly, the parameterization seems to drastically limit ice supersaturation at low temperatures in atmospheric situations, while still producing ample ice crystals. Some discussion of the realism of that result should be added.

**Authors' response:** The main reason for the higher ice number concentrations despite lower supersaturations is that our laboratory-based parameterization yields higher values of  $n_s$  at e.g. at ~110% than the P13 parameterization gives at e.g. ~130%. In addition, also with the new parameterization, supersaturations up to 120% are reached occasionally. One possible explanation for this simulated high ice formation is the contribution of updrafts, where supersaturation conditions are maintained. Nevertheless, since atmospheric measurements of supersaturations in cirrus regions seem still uncertain, and high atmospheric supersaturations are still under debate (e.g., *Peter et al.*, 2006; *Krämer et al.*, 2009), we cannot say for certain about the realism of this feature and, therefore, prefer no discussion in the current manuscript.

#### References:

Peter, T., Marcolli, C., Spichtinger, P., Corti, T., Baker, M. B. and Koop, T.: When dry air is too humid, *Science*, 314, 1399-1402, doi:10.1126/science.1135199, 2006.

Krämer, M., Schiller, C., Afchine, A., Bauer, R., Gensch, I., Mangold, A., Schlicht, S., Spelten, N., Sitnikov, N., Borrmann, S., de Reus, M., and Spichtinger, P.: Ice supersaturations and cirrus cloud crystal numbers, *Atmos. Chem. Phys.*, 9, 3505-3522, doi:10.5194/acp-9-3505-2009, 2009.

**Reviewer's comment:** Lines 21-24, but also a general comment: The major question this begs is why we should deem that hematite is representative for cirrus, and why we should deem that the lab studies are relevant for atmospheric particles? This seems like a topic in itself.

**Authors' response:** We did not select hematite because it is a major atmospheric dust component in cirrus clouds, but we chose hematite because it is a good model substance to infer  $n_s$  values over a wide  $T$  and  $RH_{ice}$  range (discussed above). The compatibility between hematite particles and desert dust particles has already been demonstrated in the first version of our manuscript (i.e., Fig. 3A and associated text on the page 16506 lines 20-25; page 16507 lines 20-22).

To further clarify, we have updated the abstract. Modifications are performed to the old text as follows:

Page 16494 lines 5-7:

Original: "The surface-scaled ice nucleation efficiencies of hematite particles, inferred by  $n_s$ , were derived from AIDA..."

→

Modified: "The ice nucleation active surface-site density ( $n_s$ ) of hematite particles, used as a proxy for atmospheric dust particles, were derived from AIDA..."

Page 16494 lines 16-19:

Original: "We implemented new  $n_s$  parameterizations into two cloud models to investigate its sensitivity and compare with the existing ice nucleation schemes towards simulating cirrus cloud properties."

→

Modified: "We implemented the new hematite-derived  $n_s$  parameterization, which agrees well with previous AIDA measurements of desert dust, into two conceptual cloud models to investigate their sensitivity to the new parameterization in comparison to existing ice nucleation schemes for simulating cirrus cloud properties."



**Reviewer's comment:** The parameterization you choose to compare to is constrained by measurements of atmospheric IN, and it notes already that the results are inconsistent with cloud chamber data for pure mineral dusts. Hence, it should be understood that this is not a new story, but a remaining mystery of sorts. This paper may shed some additional light on it due to the fact that it is hard to imagine a different situation for any pure dust aerosol, so perhaps the atmospheric measurements had some unresolved issues. Nevertheless, this paper needs to state more clearly what its goals are besides the new dust parameterization.

**Authors' response:** For clarity, we have modified the following sentence:

Page 16497 lines 26-28: “Applications of the fitted  $n_s$  parameterization derived from these measurements to atmospheric modeling simulations were also performed.” → now reads, “In addition to developing the new dust parameterizations from these AIDA measurements (Sects. 3.1-3.3), the fitted  $n_s$  parameterization was also applied to atmospheric modeling simulations (Sect. 3.4).”

In addition, we have added the following sentence on the page 16498 line 3 after “...existing parameterizations.”:

“It is important to note that the purpose of the current study is to perform a conceptual study with laboratory-synthesized hematite particles as a model aerosol for deposition ice nucleation, over a wide range of  $T$  and  $RH_{ice}$ , but not to quantify how much hematite content contributes to ice formation in cirrus clouds.”

**Reviewer's comment:** Page 16496, lines 8-10: Regarding this statement, I do not understand what is meant by Welti et al. introducing this idea. The concept of a freezing mechanism of solutions on particles at below water saturation has a history in going back to Zuberi et al. (2002), Archuleta et al. (2005) and so forth. Welti et al. referenced this earlier work (exploring it in the context of CNT), as does the present paper later in the manuscript.

**Authors' response:** We thank the reviewer's suggestion for these useful literatures (Zuberi et al., 2002; Hung et al., 2003; Archuleta et al., 2005) and are now added on the page 16496 lines 8-10:

“Recently, Welti et al. (2014) introduced the relevance of soluble components of mineral dust (i.e., Fluka kaolinite) to condensation freezing below water saturation.”

→

“Previous laboratory studies introduced the concept of a freezing mechanism of solutions on particles at below water saturation (Zuberi et al., 2002; Hung et al., 2003; Archuleta et al., 2005). More recently, Welti et al. (2014) explored the relevance of soluble components of mineral dust (i.e., Fluka kaolinite) to condensation freezing below water saturation in the context of classical nucleation theory (CNT).”

The CNT abbreviation is now used in the page 16496 line 24:

“Besides, classical nucleation theory (CNT)-based” → “Besides, CNT-based”

Added references:

Archuleta, C.M., DeMott, P.J., and Kreidenweis, S.M.: Ice nucleation by surrogates for atmospheric mineral dust and mineral dust/sulfate particles at cirrus temperatures, *Atmos. Chem. Phys.*, 5, 2617-2634, doi:10.5194/acp-5-2617-2005, 2005.

Zuberi, B., Bertram, A.K., Cassa, C.A., Molina, L.T., and Molina, M.J.: Heterogeneous nucleation of ice in  $(\text{NH}_4)_2\text{SO}_4\text{-H}_2\text{O}$  particles with mineral dust immersions, *Geophys. Res. Lett.*, 29, 1504, doi:10.1029/2001GL014289, 2002.

Hung H.-M., Malinowski, A., and Martin, S. T.: Kinetics of heterogeneous ice nucleation on the surfaces of mineral dust cores inserted into aqueous ammonium sulfate particles, *J. Phys. Chem. A.*, 107, 1296–1306, doi: 10.1021/jp021593y, 2003.

**Reviewer’s comment:** Page 16497, lines 7-9: There is no doubt that there is a need for better parameterizations for cloud models, but an issue not mentioned is if one can be certain that laboratory measurements are representative for the atmosphere. So actually, what this seems to argue for are more and better in situ measurements. Apparently, these may not be as straightforward as setting conditions in instruments and measuring INP. At least, I think the authors should be open to all possibilities.

**Authors’ response:** The reviewer makes a good point. The efforts to constrain model uncertainties from both in situ measurements and lab experiments are important and might be complementary. We updated the text in the following section to address the referee’s comment and to clarify our point.

Page 16497 lines 7-9:

Original: “Therefore, systematic laboratory measurements to develop water subsaturated ice nucleation parameterizations for the range of atmospherically relevant  $T\text{-RH}_{\text{ice}}$  conditions are needed to better represent ice nucleation processes in cloud models.”

→

Modified: “To gain insight on what triggers such deviation and to constrain model uncertainties, more and better in situ measurements are necessary (*Cziczo and Froyd, 2014*). In specific, identifying and quantifying sources, global spatio-temporal distribution and mixing-state of INPs might support to reduce model assumptions. In parallel, systematic laboratory measurements are indeed needed to develop water subsaturated ice nucleation parameterizations for the range of atmospherically relevant  $T\text{-RH}_{\text{ice}}$  conditions for a better representation of ice nucleation processes in cloud models and to support in situ measurements.”

Added reference

Cziczo, D.J. and Froyd, K.D.: Sampling the composition of cirrus ice residuals, *Atmospheric Research*, 142, 15–31, doi: 10.1016/j.atmosres.2013.06.012, 2014.

**Reviewer’s comment:** Page 16498, line 6: What is the basis for selecting hematite particles as a proxy in this case?

**Authors’ response:** Their uniform chemico-physical properties, such as shape (cubic), chemical composition ( $\text{Fe}_2\text{O}_3$ ) and size (~200, ~500 and ~1000 nm diameter), which makes them as suitable test substrates to characterize ice nucleation efficiency ( $n_i$ ) at a wide temperature range (i.e., page 16503 lines 18-25).

We have made the following minor modification on text (page 16498 line 6):

Original: “Laboratory-generated cubic hematite particles...”

→

Modified: “Laboratory-generated cubic hematite particles that have homogeneous chemico-physical properties...”

**Reviewer’s comment:** Page 16501, lines 13-14: I am a bit surprised at the selection of use of the aerosol-independent M92 scheme to represent heterogeneous nucleation when applying a dust parameterization for cirrus levels. Can you please state if the values predicted by M92 are capped at some low temperature, or is it extended far beyond its usual valid (where data were represented in the original paper) temperature range? Is there a reason that the immersion freezing parameterization for hematite was not joined to the one for deposition?

**Authors’ response:** We used the M92 parameterization only for  $T > -36$  °C (discussed above; see the authors’ response to the comment from reviewer 1 on the page 4). Immersion freezing is considered as a part of SCF (details discussed below) and incorporated in our  $n_s$ -isoline-based parameterization. Use of the M92 parameterization for  $T > -36$ °C is necessary in the model applications because hematite is a rather inefficient ice nucleus in this temperature range, where other INP (e.g., biological ice nuclei, feldspars, etc.) are likely to contribute significantly to ice formation. If the M92 parameterization was not used in this range, too much supersaturated air and supercooled water would be transported to cirrus levels, and the impact of INP in cirrus clouds would be overestimated.

**Reviewer’s comment:** Page 16501, lines 21-24: Further clarification is also needed regarding the use of P13. First, does the parameterization allow initialization otherwise in accord with the present parameterization in terms of the numbers of dust particles? Second, even if ice nucleation below water saturation is used for mineral dust particles only, does not this create some likely overlap with the M92 scheme? That is, I would expect the P13 formulation to make ice prior to homogeneous freezing temperatures, where the M92 formulation is already generating ice.

**Authors’ response:** Since we re-formulated the P13 parameterization in terms of  $n_s$  (Fig. 2c), P13 was implemented in the same way (i.e., same  $T$  and  $RH_{ice}$  ranges) as the AIDA-derived parameterization by assuming 200 dust particles per L with the identical aerosol surface area. With our approach, also no ice formation was allowed in the regime covered by M92. This makes the comparison of two parameterizations consistent, using M92 at  $T > -36$ °C.

**Reviewer’s comment:** Page 16502, line 22: Is a time step of 20s reasonable or sufficient for cirrus simulations?

**Authors’ response:** In contrast to a parcel model that actively resolves the depletion of water vapor through heterogeneous ice formation, we use the parameterization-scheme of *Kärcher et al.* (2006) to parameterize the processes on small time scales, such as depletion of water vapor. *Kärcher et al.* (2006) demonstrated the implementation of their scheme into a global model with much longer time steps (~30 min).

For clarity, we now added the following sentence at the end of section 2.3.2 (page 16503 line 8):

“The latter was used to parameterize the competition of water vapor between homogeneous and heterogeneous freezing”

Reference:

Kärcher, B., Hendricks, J., and Lohmann, U.: Physically based parameterization of cirrus cloud formation for use in global atmospheric models, *J. Geophys. Res.*, 111, D01205, doi:10.1029/2005JD006219, 2006.

**Reviewer’s comment:** Page 16504, lines 23-25: Could you say a little more about how immersion freezing data is used to “constrain” fitting curves? Because immersion freezing is requisite at the warmer

temperatures? Or because you consider SCF as a subset of immersion freezing? Yet, you have not yet introduced the concept of SCF in the paper to this point.

**Authors' response:** We thank the referee to raise this important point. We now describe how immersion freezing data are used on the page 16504 lines 23-25:

Original: “Previous AIDA measurements of immersion freezing (i.e., INUIT04\_13 and INUIT01\_28 from *Hiranuma et al.*, 2014) are also shown and used to constrain the fitted curves.”

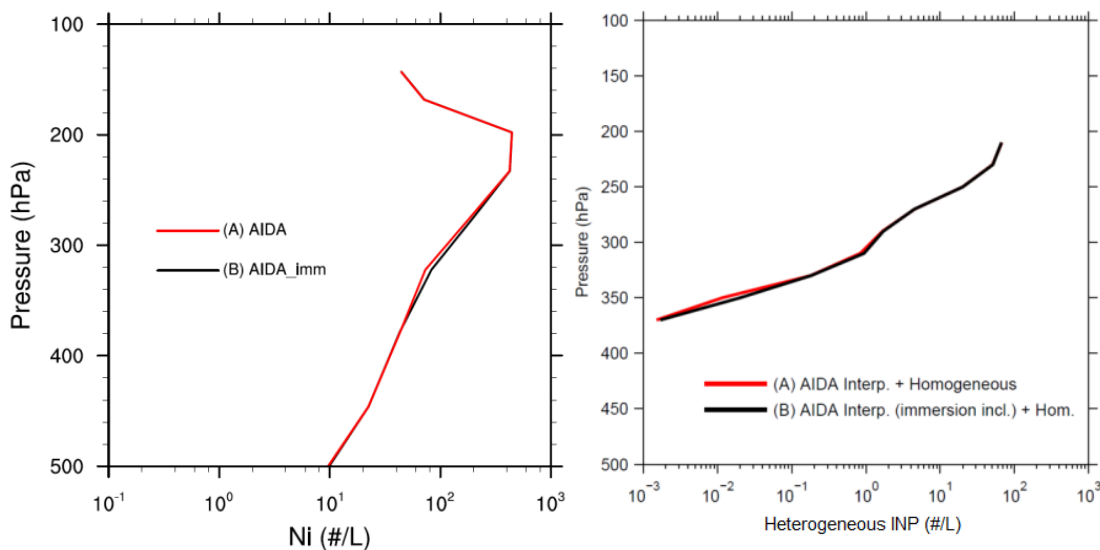
→

Modified: “Previous AIDA results of two immersion freezing experiments (i.e., INUIT04\_13 and INUIT01\_28 from *Hiranuma et al.*, 2014) are also shown on the water saturation line and used to constrain the fitted curves because immersion freezing is considered part of isolines. Since the  $n_s$  values presented in Fig. 3 of *Hiranuma et al.* (2014) only extends up to  $\sim 10^9$  m<sup>-2</sup>, the data points of higher  $n_s$  values were extrapolated based on the observed values from two measurements.”

The review is correct in pointing out that SCF is considered as a subset of immersion freezing. We now updated the first paragraph on the page 16511:

“As described in the previous section (Sect. 3.1), deposition mode freezing cannot solely explain the  $n_s$ -isoline observation below water saturation ( $-50$  °C < T <  $-36$  °C in Fig. 2). Although we presumed that SCF acts as a subset of immersion freezing and plays an important role in this region, further insight and evidence of SCF beyond cloud simulation chamber observations are required to correctly understand the contributions of both homogeneous and heterogeneous nucleation. High-resolution microscopic techniques with an integrated continuous cooling setup are needed to visualize the freezing process of a single particle and to fully understand the complex freezing processes involved in SCF on particle surfaces.”

We have evidence that both including immersion freezing data and not including them (but extrapolating the  $n_s$ -isoline fit to water saturation line) can reproduce similar (almost identical) simulation results in the simulations with SCAM5 and COSMO (please see figures below).



**Extra Figure.** Comparison of two parameterizations (i.e., including immersion data vs. extrapolating without immersion data) in monthly mean profiles of the simulated in-cloud ice crystal number

concentrations with SCAM5 (left) and the heterogeneous INP number concentration averaged over two days with COSMO (right).

We feel that we provide the definition of SCF given in right place (Sect. 3.1 on the page 16505 lines 14-25) and no earlier discussion is necessary.

**Reviewer's comment:** Page 16505, line 9: I suggest replacing “while concurrent” with “during”

**Authors' response:** Corrected.

**Reviewer's comment:** Page 16505, line 14: Considering this sentence ending, “: : pointed to a new freezing process in this study” I believe that “point” would be more appropriate. However, there seems a basic problem in saying it is a new freezing process, when what is imagined is something much like what has been discussed explicitly in recent papers and has been alluded to in some previous ones. Should it say that these results appear to support the existence of a pore or surface freezing process, as discussed in recent literature (e.g., Marcolli, 2014). Then move on to define it as SCF, rather than PCF.

**Authors' response:** We agree. We now rephrased the sentence on the page 16505 lines 12-14 as:

“Therefore, other microphysical processes at the particle surface and/or perhaps even within the bulk phase may be responsible for this  $T$ -dependent behavior and these results appear to support the existence of a pore or surface freezing process, as discussed in recent literature (e.g., Marcolli, 2014).”

**Reviewer's comment:** Page 16506: I must question the semantics of what can be called “atmospheric dust particles” because I am not terribly convinced that the hematite results encapsulated by  $n_s$  fits show that they are comparable to actual atmospheric dust, but rather to soil dust samples brought into the laboratory. Are any of the referenced studies, for any temperature regime, actual measurements of atmospheric dust, rather than surrogates for such?

**Authors' response:** Matsuki *et al.* (2010) studied atmospheric dust particles. More specifically, the authors deduced that airborne dust residuals collected through the counter virtual impactor (Ogren *et al.*, 1985) during flights in stratocumulus clouds over Niger contained hematite.

Reference:

Ogren, J. A., Heintzenberg J., and Charlson R. J.: In-situ sampling of clouds with a droplet to aerosol converter, *Geophys. Res. Lett.* 12, 121–124, doi: 10.1029/GL012i003p00121, 1985.

**Reviewer's comment:** Page 16506, line 9: “are” compared.

**Authors' response:** Corrected.

**Reviewer's comment:** Page 16506, line 16: Is “mobile” the right word for such ice nuclei counters? Mobile implies that they move, rather than the fact that they are movable or able to be installed on aircraft. Perhaps “portable”?

**Authors' response:** Thank you. We agree and corrected.

**Reviewer's comment:** Page 16508, lines 3-5: The lower bound was explained, but not the upper. What controls the upper bound, why physically does  $n_s$  remain constant up to the water saturation line, and why

presumably? It is explained rather obtusely at present. Does it mean simply that experimental data does not exist in this regime?

**Authors' response:** The answer is yes. Within our experimental conditions, the highest estimated  $n_s$  was  $\sim 10^{12} \text{ m}^{-2}$  before the peak  $\text{RH}_{\text{ice}}$  (i.e., Fig. 2), even accounting for continuous increase in  $n_s$  after depletion of supersaturation (i.e., Fig. S2), and we simply did not want to extrapolate the isoline fit to 'unexplored' region.

We have now rephrased the sentence (page 16508 lines 3-5) to:

“Above the upper bound of  $10^{12} \text{ m}^{-2}$ ,  $n_s$  presumably remains constant up to the water saturation line in  $T - \text{RH}_{\text{ice}}$  space (no experimental data is available in this range).”

**Reviewer's comment:** Page 16509: Various here, the “three” and “four” parameterizations are mentioned. Please clarify.

**Authors' response:** To clarify our study cases, we have modified and updated the texts in the following sections:

Page 16509 lines 9-13:

Original: “These include the pure homogeneous ice nucleation case (Simulation A), three cases with contributions from both the homogeneous and heterogeneous ice nucleation (hereafter combined case) described in Fig. 4 (Simulations B, C and D) and the simulation of the different lower boundaries of  $\text{RH}_{\text{ice}}$  ( $\text{RH}_i^*$ , Simulation D).”

→

Modified: “These include (Case 1) the pure homogeneous ice nucleation case, (Case 2-4) cases with contributions from both homogeneous and heterogeneous ice nucleation (hereinafter referred to as the combined case) described in Fig. 4a-c (corresponding to Simulations A, B and C) and (Case 5) the simulation of the different lower boundaries of  $\text{RH}_{\text{ice}}$  ( $\text{RH}_i^*$ , Simulation D).”

Page 16509 lines 18-20:

Original: “The differences between the four parameterizations used in this study are small for both the combined cases and the pure heterogeneous cases.”

→

Modified: “The differences between the three parameterizations derived from AIDA measurements, corresponding to Simulations A, B and D, are small for both the combined case and the pure heterogeneous ice nucleation case as presented in Fig. 6.”

Page 16509 line 25:

Original: “The three parameterizations have largest differences...”

→

Modified: “The three parameterizations (i.e., Simulations A, B and D) have largest differences...”

**Reviewer's comment:** Page 16510, COSMO simulations: I find a lot missing in the discussion here. First, the averaging used to obtain the results is not totally clear. What defines a cloudy area for the results shown in Figures 7 and 8? Does it imply that areas with very low ice content and low ice concentrations are averaged along with others of higher optical depth or higher ice water content across the domain? The lower ice concentrations in P13, despite the inclusion of homogeneous freezing are striking and somewhat

surprising unless the small regions where stronger ice formation occurs (e.g., homogeneous freezing regions) are averaged out, while the higher values in the AIDA-based parameterizations surprise me if they are averaged over all cloudy parcels, even at low ice supersaturations.

### **Authors' response:**

We thank the reviewer for pointing out that this discussion was too condensed and partly misleading. Regarding the averaging conditions, we have applied the following procedure in order to obtain consistent results for the different simulations:

The INP concentrations as well as  $T$  and  $RH_{ice}$  conditions allowing for hematite to nucleate through deposition mode, i.e.  $T < -36^\circ\text{C}$  and  $RH_{ice} > 100\%$ , are extracted and binned in pressure intervals for subsequent averaging, which yields the data in Figure 7. This averaging procedure was implemented for both the AIDA-based parameterization and P13. In case of P13, this leads to averaging also over zeros, when temperatures are below  $-36^\circ\text{C}$ , but the supersaturation is low enough that the parameterization returns  $n_s = 0$  (white areas of Figure 4C).

Note that Fig. 7 shows only the heterogeneous INP concentration. Although contained in the simulation and calculated right afterwards heterogeneous ice formation, the homogeneously formed ice is not contained in the mean values of Figure 7. Here we compare only ice that is formed by deposition nucleation, rather than “total” ice occurring in the model. In this way, the effects of sedimentation, advection and turbulent diffusion of ice crystals (that had been formed earlier in the model and may be present in  $T < -36^\circ\text{C}$  and  $RH_{ice} > 100\%$  regions due to transport) are disregarded in order to extract the heterogeneous ice formation.

We have modified the text on the page 16510 lines 9-13:

Original: “ $N_{ice}$  was spatially averaged over all cloudy areas of the model domain for freezing conditions of cubic hematite particles. As shown in Fig. 7, the mean  $N_{ice}$  resulting from the parameterization based on P13 is smaller than that from the AIDA  $n_s$ -isoline-based parameterization by more than two orders of magnitude.”

→

Modified: “ $N_{ice}$  was spatially averaged over all areas of the model domain which in principle allow for deposition nucleation in our simulations, i.e. conditions below  $-36^\circ\text{C}$  and above 100%  $RH_{ice}$ . Because not always  $n_s$  is larger than zero (white areas of Fig. 2), also areas without ice formation are contained. It is also noteworthy that only purely heterogeneous ice formation is presented rather than the total ice occurring in the model. As shown in Fig. 7, the mean  $N_{ice}$  resulting from the parameterization based on P13 is smaller than that obtained from the AIDA  $n_s$ -isoline-based parameterization by more than two orders of magnitude. This large difference results predominantly from the inactivity of P13 at low  $RH_{ice}$ .”

The x-axis in Fig. 7 and caption have been modified:

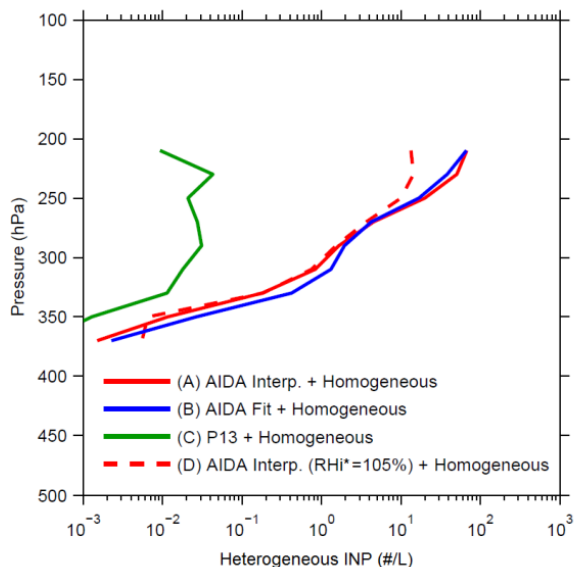


**Figure 7.** The mean heterogeneous INP number concentrations simulated in COSMO.

**Reviewer's comment:** Next, the results not only show a vast difference between the domain averaged ice crystal concentrations, but the relative picture of maximum supersaturation evident in Figure 8 is drastically different. If I follow this correctly, it would be highly unlikely to find an area supersaturated with respect to ice by more than 20

**Authors' response:** Our presentation is correct. Most of ice formation, in case of using AIDA-derived parameterization, is triggered below  $RH_{ice}$  120% (Fig. 8A) owing to our  $n_s$  parameterization which shows non-negligible ice formation even at low  $RH_{ice}$  and simulated atmospheric conditions in COSMO.

**Reviewer's comment:** Page 16510, last sentence: The data in P13 are clearly limited at lower temperatures. That paper acknowledged this issue and also discussed discrepancies between field and laboratory data at temperatures below  $-35$  °C, offering some speculation about this. Can you say that your results confirm these things and can you speak to whether or not the modeling provides any new insights?

**Authors' response:** What we see from the results of both models is that the modeled ice concentrations are very sensitive to deposition nucleation at low temperatures when heterogeneous INPs (hematite particles in this study) compete with homogeneous freezing. Because the low supersaturations have a high frequency of occurrence in the atmosphere, it is highly desirable that atmospherically relevant IN (mineral dust and others) are described more precisely with respect to their deposition nucleation ability in the cirrus regime.

**Reviewer's comment:** Page 16511, lines 14-18: I wonder if the discrepancies between the parameterizations noted here do not actually highlight most the need for more high quality atmospheric measurements of INP's in the upper troposphere. This is what stands out to me at least. The laboratory measurements seem consistent.

**Authors' response:** The authors believe that in situ measurements of INPs, such as the number concentration and the types of INPs, can constrain lab based parameterizations. Though direct observation of the aerosol freezing mechanism in the upper troposphere where coincides with the low water vapor pressure (Cziczo and Froyd, 2014), investigating chemical characterization of cirrus residual particles can



give a crucial hint and promote the investigation of ice formation mechanism by using laboratory instruments (e.g., AIDA).

We have rephrased the sentences on the page 16511 lines 14-23:

Original: “Substantial differences between the empirical approach of P13 and our parameterization developed in this study are presumably attributed to the difference in lab- or field data, highlighting the need for further characterizations of atmospherically relevant substrates and their ice nucleation activities in laboratory settings. Nevertheless, *Niemand et al.* (2012) demonstrated that different dusts exhibit similar  $n_s$  in immersion mode freezing and perhaps such a similarity remains true for deposition mode ice nucleation. In fact, comparison between our AIDA  $n_s$ -based parameterization with hematite particles and *Möhler et al.* (2006) with ATD and SD2 (Fig. 3a) provides indication on the validity of the assumption to treat all dust as hematite in deposition mode.”

→

Modified: “However, it should be noted that there is some evidence for the atmospheric relevance and applicability of the new parameterization. First of all we demonstrated that the new  $n_s$  parameterization based on the experiments with hematite particles agrees well with previous literature results for mineral dust aerosol (e.g., *Möhler et al.*, 2006; *Welti et al.*, 2009; *Köhler et al.*, 2010). Second, *Niemand et al.* (2012) demonstrated that different dusts exhibit similar  $n_s$  in immersion mode freezing and perhaps such a similarity remains true for the deposition mode ice nucleation of desert dusts. Lastly, the comparison between the observed profile of ice crystal number concentrations and the simulated ones (Figs. 5 and 6) also suggests the validity of the new parameterization. These premises must be further examined in comparing to atmospherically relevant substrates (fresh and aged ones) and their ice nucleation activities in laboratory settings. In situ INP measurements, such as the number concentration and the types of INPs, at the upper troposphere can also help to constrain the parameterization.”

**Reviewer’s comment:** Page 16512, lines 14-16: I did not note anywhere in the paper where a hypothesis for the appearance of an RH<sub>ice</sub>-dependent ice nucleation below -60 °C was discussed. Can you suggest anything?

**Authors’ response:** Discussed on the page 16504 lines 25-27:

For clarity, we have added “(i.e., RH<sub>ice</sub>-dependent ice nucleation regime)” in the end of this sentence (page 16504 lines 25-27):

“Figure 2 shows several important features of  $n_s$ -isoline curves. First, below -60 °C,  $n_s$ -isolines showed an increase in RH<sub>ice</sub> required to maintain a constant  $n_s$  (i.e.,  $n_s > 2.5 \times 10^8 \text{ m}^{-2}$ ) with decreasing  $T$  (i.e., RH<sub>ice</sub>-dependent ice nucleation regime).”

**Reviewer’s comment:** Last sentence: Can you comment on whether or not you believe that the stronger ice nucleation at limited ice supersaturations on the basis of the new parameterization is realistic for the atmosphere? How might this be examined?

**Authors’ response:** How strong ice nucleation at lower RH<sub>ice</sub> can be examined and quantified by conducting ‘direct’ measurements of INP concentration as a function of  $T$  and RH<sub>ice</sub>. This could ultimately verify how realistic the lab results are for the atmosphere. Nonetheless, both experimental and model results (Fig. 2 and 8A) suggest the new parameterization to induce substantial ice formation even at low RH<sub>ice</sub>. Hence, the new parameterization strongly suggests the role of  $T$  and more ice nucleation when compared to the existing empirical parameterization, presumably allowing more ice activation under water subsaturated conditions.

**Additional revision:** In addition to addressing the reviewer's comments, other editorial corrections (major and non-miscellaneous ones) were made and listed above on the pages 11-13 of authors' responses.

All relevant changes made in the manuscript are indicated by the highlighted sections in yellow (as of September 30 2014) and green (added on October 1, 2014) below.

1 **A Comprehensive Parameterization of Heterogeneous Ice Nucleation of Dust Surrogate:**  
2 **Laboratory Study with Hematite Particles and Its Application to Atmospheric Models**

3  
4 Naruki Hiranuma<sup>a,\*</sup>, Marco Paukert<sup>a</sup>, Isabelle Steinke<sup>a</sup>, Kai Zhang<sup>b</sup>, Gourihar Kulkarni<sup>b</sup>,  
5 Corinna Hoose<sup>a</sup>, Martin Schnaiter<sup>a</sup>, Harald Saathoff<sup>a</sup> and Ottmar Möhler<sup>a</sup>

6  
7 <sup>a</sup>*Institute for Meteorology and Climate Research – Atmospheric Aerosol Research,*  
8 *Karlsruhe Institute of Technology, Karlsruhe, Germany.*

9 <sup>b</sup>*Atmospheric Science and Global Change Division,*  
10 *Pacific Northwest National Laboratory, Richland, Washington, USA*

11  
12 \*Corresponding Author. E-mail: seong.moon@kit.edu

13  
14  
15  
16  
17  
18  
19  
20  
21  
22  
23  
24  
25  
26  
27  
28 Manuscript in preparation for *Atmospheric Chemistry and Physics*  
29 **ACP - Special Issue: Results from the ice nucleation research unit (INUIT)**  
30

31 October 1, 2014

32 **Abstract**

33

34 A new heterogeneous ice nucleation parameterization that covers a wide temperature  
35 range (-36 to -78 °C) is presented. Developing and testing such an ice nucleation  
36 parameterization, which is constrained through identical experimental conditions, is important to  
37 accurately simulate the ice nucleation processes in cirrus clouds. The ice nucleation active  
38 surface-site density ( $n_s$ ) of hematite particles, used as a proxy for atmospheric dust particles,  
39 were derived from AIDA (Aerosol Interaction and Dynamics in the Atmosphere) cloud chamber  
40 measurements under water subsaturated conditions. These conditions were achieved by  
41 continuously changing the temperature ( $T$ ) and relative humidity with respect to ice ( $RH_{ice}$ ) in the  
42 chamber. Our measurements showed several different pathways to nucleate ice depending on  $T$   
43 and  $RH_{ice}$  conditions. For instance, almost  $T$ -independent freezing was observed at  $-60\text{ °C} < T < -$   
44  $50\text{ °C}$ , where  $RH_{ice}$  explicitly controlled ice nucleation efficiency, while both  $T$  and  $RH_{ice}$  played  
45 roles in other two  $T$  regimes:  $-78\text{ °C} < T < -60\text{ °C}$  and  $-50\text{ °C} < T < -36\text{ °C}$ . More specifically,  
46 observations at  $T$  lower than  $-60\text{ °C}$  revealed that higher  $RH_{ice}$  was necessary to maintain a  
47 constant  $n_s$ , whereas  $T$  may have played a significant role in ice nucleation at  $T$  higher than  $-50$   
48  $\text{°C}$ . We implemented the new hematite-derived  $n_s$  parameterization, which agrees well with  
49 previous AIDA measurements of desert dust, into two conceptual cloud models to investigate  
50 their sensitivity to the new parameterization in comparison to existing ice nucleation schemes for  
51 simulating cirrus cloud properties. Our results show that the new AIDA-based parameterization  
52 leads to an order of magnitude higher ice crystal concentrations and to an inhibition of  
53 homogeneous nucleation in lower temperature regions. Our cloud simulation results suggest that  
54 atmospheric dust particles that form ice nuclei at lower temperatures, below  $-36\text{ °C}$ , can  
55 potentially have a stronger influence on cloud properties, such as cloud longevity and initiation,  
56 compared to previous parameterizations.

57 **1. Introduction**

58

59 Ice clouds represent a significant source of uncertainty when predicting the Earth's  
60 climate change according to the recent Intergovernmental Panel on Climate Change report (i.e.,  
61 Chapter 7 of IPCC, 2013; Boucher et al., 2013). Rare airborne particles that can act as ice  
62 nucleating particles (INPs) at supercooled temperatures indirectly influence the Earth's forcing  
63 by changing microphysical properties of ice clouds, such as reflectivity, longevity and  
64 precipitation. However, understanding ice cloud formation over a wide range of atmospherically  
65 relevant temperatures and humidity is challenging (e.g., DeMott et al., 2011; Murray et al.,  
66 2012), and our knowledge of ice formation through various nucleation modes is still scarce and  
67 limited, such that the ice nucleation processes are currently very poorly represented in global  
68 climate models (e.g., Hoose et al., 2010; Liu and Penner, 2005). In particular, heterogeneous ice  
69 nucleation processes proceed through various modes including deposition nucleation,  
70 immersion-, condensation- and contact freezing (Chapter 9 of Pruppacher and Klett, 1997; Vali,  
71 1985). Briefly, deposition mode induces ice formation when water vapor is directly deposited  
72 onto the INP, immersion and condensation freezing can induce ice formation when freezing is  
73 initiated by the INP immersed within the supercooled droplet or solution droplet, and contact  
74 freezing can initiate at the moment when an INP comes into contact with a supercooled droplet.

75 A global model simulation of INPs in tropospheric clouds showed that more than 85% of  
76 heterogeneous ice nucleation results from freezing of supercooled cloud droplets, in which INPs  
77 are either immersed or condensed (Hoose et al., 2010). However, freezing mechanisms in cirrus  
78 clouds are still uncertain (e.g., Sassen and Khvorostyanov, 2008). It is understood that various  
79 INPs can nucleate ice at water subsaturation and a range of supercooled temperature conditions  
80 as comprehensively illustrated in Fig. 2 of Hoose and Möhler (2012). The potential importance  
81 of ice nucleation under ice supersaturated conditions below the homogeneous freezing threshold  
82 line (i.e., Koop line; Koop et al., 2000; Ren and MacKenzie, 2005) has already been proved in  
83 earlier studies, suggesting the need for further investigations in the water subsaturated region.  
84 For example, Christenson (2013) experimentally showed that the capillary condensation of  
85 supercooled liquid on surface defects facilitated subsequent homogeneous nucleation and growth  
86 of ice below water saturation. Marcolli (2014) suggested that the inverse Kelvin effect below  
87 water saturation helps to form water in pores or cavities and hypothesized that this condensate

88 could freeze through the homogeneous- or immersion mode freezing. This freezing mechanism  
89 was referred to as pore condensation and freezing. Previous laboratory studies introduced the  
90 concept of a freezing mechanism of solutions on particles at below water saturation (Zuberi *et al.*,  
91 2002; Hung *et al.*, 2003; Archuleta *et al.*, 2005). More recently, Welts *et al.* (2014) explored the  
92 relevance of soluble components of mineral dust (i.e., Fluka kaolinite) to condensation freezing  
93 below water saturation in the context of classical nucleation theory (CNT). Further, recent  
94 aircraft-based field observations suggested that predominant heterogeneous ice formation at  
95 cirrus temperatures occurs under water subsaturated conditions, in particular when  $RH_{ice}$  is  
96 below 140% (Cziczo *et al.*, 2013). In addition, Storelvmo and Herger (2014) demonstrated that  
97 forward modeling simulation with 50% of the mineral dust particles acting as INPs was in good  
98 agreement with an observation reported by Cziczo *et al.* (2013). Another airborne observation  
99 during an Asian mineral dust event suggested that ice nucleation in cirrus clouds occurs under  
100 water subsaturation conditions below 130%  $RH_{ice}$  (Sakai *et al.*, 2014).

101 Previously, empirical descriptions given in Meyers *et al.* (1992, hereinafter referred to as  
102 M92) were derived from the limited field measurements of ice nuclei concentrations measured at  
103  $-23\text{ }^{\circ}\text{C} < T < -7\text{ }^{\circ}\text{C}$  and  $102\% < RH_{ice} < 125\%$ . Recently, Phillips *et al.* (2008, 2013) empirically  
104 parameterized the heterogeneous ice nucleation of various types of aerosols as a function of  
105 humidity ( $RH_{ice} > 100\%$ ) and temperature conditions (0 to  $-100\text{ }^{\circ}\text{C}$ ). Besides, CNT-based ice  
106 nucleation descriptions have also been widely used and implemented in cloud models (e.g.,  
107 Barahona and Nenes, 2009a and 2009b; Kärcher and Lohmann, 2003; Khvorostyanov and Curry,  
108 2004). These parameterizations can predict different cloud properties for identical environmental  
109 conditions. For example, Barahona *et al.* (2010) showed that the ice crystal number can vary by  
110 up to an order of magnitude in a global chemical transport model depending on the choice of the  
111 heterogeneous ice nucleation parameterization. The authors found the lowest global mean ice  
112 crystal concentration from the parameterization of Phillips *et al.* (2008). Moreover, sensitivity of  
113 ice cloud properties to the parameterization was observed by Liu *et al.* (2012). They showed that  
114 the heterogeneous INP number concentration obtained from a CNT-based parameterization is  
115 typically higher by several factors than that of Phillips's parameterization under identical test  
116 conditions. To gain insight on what triggers such deviation and to constrain model uncertainties,  
117 more and better in situ measurements are necessary (Cziczo and Froyd, 2014). In specific,  
118 identifying and quantifying sources, global spatio-temporal distribution and mixing-state of INPs

119 might support to reduce model assumptions. In parallel, systematic laboratory measurements are  
120 indeed needed to develop water subsaturated ice nucleation parameterizations for the range of  
121 atmospherically relevant  $T$ -RH<sub>ice</sub> conditions for a better representation of ice nucleation  
122 processes in cloud models and to support in situ measurements.

123 Recently, *Hoose and Möhler* (2012) compiled previously reported aerosol-specific  
124 heterogeneous freezing efficiencies from laboratory experiments based on a single-parameter,  $n_s$   
125 (e.g., *Niemand et al.*, 2012; *Connolly et al.*, 2009). In addition, the authors formulated ice  
126 nucleation efficiency by evaluating aerosol-specific “singular” freezing onsets when or after  
127 specific ambient conditions were met. Such time-independent and surface area-scaled  $n_s$   
128 formulations can be further adapted to comprehensively assess the ice nucleation in a wide range  
129 of atmospherically relevant  $T$ -RH<sub>ice</sub> conditions. Accordingly, the  $n_s$  concept was adapted to  
130 deposition nucleation at low temperatures (up to -80 °C).

131 Within the framework of Ice Nucleation research UnIT (INUIT), we comprehensively  
132 investigated the ice nucleation efficiency of pristine cubic hematite particles as a model proxy for  
133 atmospheric dust particles. Hematite is used as an example of atmospheric mineral dust particles,  
134 which can also be found in the form of cloud-borne particles in shallow stratocumulus clouds  
135 (*Matsuki et al.*, 2010). Natural hematite often exists in supermicron-sized silt particles and  
136 accounts for a few percent of the total dust particle mass (*Claquin et al.*, 1999). Ice nucleation  
137 efficiencies of cubic hematite particles were measured using the AIDA cloud chamber. We also  
138 re-examined the previously reported AIDA results of hematite ice nucleation (*Hiranuma et al.*,  
139 2014; *Skrotzki et al.*, 2013) and combined them with the results from this work in order to  
140 examine the ice nucleation efficiency of hematite particles in the temperature range between -36  
141 and -78 °C. In addition to developing the new dust parameterization from these AIDA  
142 measurements (Sects. 3.1-3.3), the fitted  $n_s$  parameterization was also applied to atmospheric  
143 modeling simulations (Sect. 3.4). We implemented the parameterization in the Single column  
144 version of the Community Atmospheric Model version 5 (SCAM5, *Neale et al.*, 2010) and the  
145 Consortium for Small-scale Modeling (COSMO, *Baldauf et al.*, 2011; *Doms et al.*, 2011)  
146 models to assess the newly developed parameterization and compare them with existing  
147 parameterizations. It is important to note that the purpose of the current study is to perform a  
148 conceptual study with laboratory-synthesized hematite particles as a model aerosol for deposition

149 ice nucleation, over a wide range of  $T$  and  $RH_{ice}$ , but not to quantify how much hematite content  
150 contributes to ice formation in cirrus clouds.



151 **2. Method**

152

153 **2.1. Description of hematite particles**

154

155 Laboratory-generated cubic hematite particles that have homogeneous chemico-physical  
156 properties were used as a proxy for atmospheric dust particles. These particles had a uniform  
157 composition, morphology and well-defined surface area. Hence, they are suited well for  
158 investigating  $T$ - $RH_{ice}$ -dependent ice nucleation efficiency and relating it to the surface area  
159 (Hiranuma *et al.*, 2014). Detailed information on the manufacturing process of cubic hematite  
160 particles is available elsewhere (Sugimoto and Sakata, 1992). Three different sizes of quasi-  
161 monodispersed hematite particles (~200, ~500 and ~1000 nm diameter, respectively) were used  
162 in this work. The morphology and size of the hematite particles were characterized by scanning  
163 electron microscopy and determined based on an equivalent circle diameter derived from the  
164 observed 2D particle projection area (Vragel, 2009; Hiranuma *et al.*, 2014). A Small-Scale  
165 Powder Disperser (SSPD, TSI, Model 3433) was used to dry-disperse the quasi-monodispersed  
166 hematite particles into the AIDA vessel as demonstrated in Skrotzki *et al.* (2013).

167

168 **2.2. AIDA cooling expansion**

169

170 The AIDA expansion freezing experiments were achieved by mechanical pumping  
171 (Möhler *et al.*, 2003). Mechanical pumps can be operated at different pumping speeds simulating  
172 atmospherically relevant adiabatic cooling of rising air parcels in the cylinder of 84 m<sup>3</sup> in volume  
173 (i.e., 7 m height x 4 m width thermally conductive aluminum vessel) installed inside the  
174 thermostatic housing. For this study, a cooling rate of 5 °C min<sup>-1</sup> was typically applied at the  
175 beginning. Then, the cooling rate decreased to <0.1 °C min<sup>-1</sup> within 400 s for each pumping  
176 expansion experiment, which was mainly due to an increasing heat flux from the chamber walls.  
177 Afterwards, an almost constant temperature was maintained by the stirred and well-mixed  
178 volume of the cold chamber. During the experiment, the pressure in the vessel decreased from  
179 1000 to 800 mb.

180 The mean gas temperature in the AIDA vessel was determined by five thermocouples  
181 installed at different vertical levels. The sensors of these thermocouples were located about 1 m

182 off the vessel wall and, thus, fully exposed to the chamber air. Stirring of the air by the  
183 mechanical ventilator prior to and during pumping ensured a homogeneous temperature  
184 distribution in the vessel of  $\pm 0.3$  °C (Möhler *et al.*, 2003). The relative humidities with respect  
185 to water ( $RH_{\text{water}}$ ) and  $RH_{\text{ice}}$  were determined with an accuracy of  $\pm 5\%$  using the mean gas  
186 temperature and the mean water vapor concentration. The water vapor concentrations were  
187 measured in situ by tunable diode laser (TDL) water vapor absorption spectroscopy throughout  
188 the expansion experiments. Since this direct long path absorption technique is described and  
189 evaluated in detail in other publications (Fahey *et al.*, 2014; Skrotzki *et al.*, 2013), no further  
190 information is given here.

191 Under atmospheric pressure, prior to each expansion experiment, a combination of a  
192 Scanning Mobility Particle Sizer (SMPS, TSI, Model 3080 DMA and Model 3010 condensation  
193 particle counter), an Aerosol Particle Sizer (APS, TSI, Model 3321) and a condensation particle  
194 counter (CPC, TSI, Model 3076) collectively measured the total number and size distribution of  
195 aerosols at the horizontally extended outlet of the AIDA chamber. Subsequently, the total aerosol  
196 surface area was estimated as presented in Hiranuma *et al.* (2014). During expansion, we  
197 quantified the ice nucleation of hematite particles with two different light scattering instruments:  
198 an optical particle counter welas (PALAS, Sensor series 2300 and 2500) (Benz *et al.*, 2005) and  
199 SIMONE (German acronym of Streulicht-intensitätsmessungen zum optischen Nachweis von  
200 Eispartikeln, which translates to the scattering intensity measurement for the optical detection of  
201 ice; Schnaiter *et al.*, 2012). More details on the application of this specific combination of two  
202 instruments for the AIDA ice nucleation experiments are given in Hiranuma *et al.* (2014).

203

### 204 2.3. Ice nucleation parameterization and modeling

205

206 The size-independent singular ice nucleation efficiency,  $n_s$ , was calculated by  
207 normalizing the observed AIDA ice crystal concentration ( $N_{\text{ice}}$ ) to the total surface area of  
208 aerosols, which can be calculated by multiplying the surface area of an individual particle ( $S_i$ ) by  
209 the total number concentration of aerosols ( $N_{\text{ae}}$ ) (e.g., Niemand *et al.*, 2012; Hoose and Möhler,  
210 2012). For size-selected hematite particles, this linear approximation (i.e.,  $n_s = (-\ln(1-\alpha))/S_i \sim$   
211  $\alpha/S_i$ ) was valid independent of the ice active number fraction ( $\alpha = N_{\text{ice}}/N_{\text{ae}}$ ). An overestimation of  
212 ice due to the use of linear approximation only amounted up to about a factor of three at  $n_s \leq 10^{12}$

213  $\text{m}^{-2}$ . Subsequently, the  $n_s$  values estimated for the wide range of experimental conditions ( $-36\text{ }^\circ\text{C}$   
214  $< T < -78\text{ }^\circ\text{C}$  and  $100\% < \text{RH}_{\text{ice}} < \text{water saturation}$ ) were used to depict and fit constant  $n_s$  contour  
215 lines. Here, these lines are referred to as the  $n_s$ -isolines or simply as the isolines.

216 The isoline-based parameterizations were derived (see section 3.3) and then implemented  
217 in two atmospheric models (a single-column version of a global scale model and a convection  
218 resolving model, see Sect 2.3.1. and 2.3.2. for model descriptions). The unique advantages of the  
219 use of both models in this study are (1) to demonstrate that our AIDA  $n_s$ -based parameterization  
220 can be directly applied on different scales of atmospheric models and (2) to estimate the number  
221 of ice crystals simulated in two different atmospheric scenarios that complement each other and  
222 cover a wide range of atmospheric temperature and saturation conditions (ice formation at higher  
223  $\text{RH}_{\text{ice}}$ , up to  $\sim 180\%$ , and lower  $T$ , down to  $\sim -70\text{ }^\circ\text{C}$ ). More specifically, the former represents a  
224 finely resolved parameterization-oriented model embedded in the global model while the latter is  
225 a more physically based high-resolution grid scale model, typically used to analyze small scale  
226 complex systems for a fundamental understanding of ice formation. Altogether, results from two  
227 independent models were examined for a detailed modeling of atmospheric ice formation on all  
228 scales.

229 The mean size and surface area of hematite particles were prescribed with an assumption  
230 that either these particles are spherical and have a mean particle diameter of 1000 nm or the size  
231 of these particles follows a lognormal distribution, with a mean volume-equivalent diameter of  
232  $\sim 1000\text{ nm}$  ( $\sigma_g = 1.05$ ), which is consistent with the AIDA experiments described earlier  
233 (Hiranuma *et al.*, 2014). The cloud microphysical sensitivity of these two size treatments was  
234 characterized. In addition, sensitivity simulations of two lower boundaries of  $\text{RH}_{\text{ice}}$  (i.e., 100 vs.  
235 105%) were also carried out. This sensitivity analysis was specifically useful to examine  
236 uncertainty involved in the TDL measurement ( $\text{RH}_{\text{ice}} \pm 5\%$ ) concerning the condensed  $n_s$  spacing  
237 (up to several orders of magnitude) in a narrow  $\text{RH}_{\text{ice}}$  range and a certain  $T$  region. In both  
238 models, hematite particle number concentrations are given to be  $200\text{ L}^{-1}$ , which is about the  
239 average dust concentration simulated by the SCAM5 model over the Southern Great Plain (SGP)  
240 site in springtime. Since the  $n_s$ -isoline parameterization tested in this study is applicable at  $T$   
241 below  $-36\text{ }^\circ\text{C}$ , an additional parameterization was used to simulate ice formation of background  
242 particles at  $T > -36\text{ }^\circ\text{C}$ , namely, the aerosol-independent M92 scheme. These parameterizations  
243 were combined to ensure more atmospherically relevant processes and conditions (e.g.,

244 distributions of water vapor) when compared to the application of the  $n_s$ -isoline parameterization  
245 alone.

246 To better understand to what an extent the AIDA  $n_s$ -based parameterization differs from  
247 other parameterizations commonly used in atmospheric models, the existing empirical  
248 parameterization of heterogeneous ice nucleation by Phillips *et al.* (2013, hereinafter denoted as  
249 P13) was implemented as well. The P13 scheme reflects the aerosol specific ice nucleation. In  
250 particular, the contribution of mineral dust with the background troposphere baseline surface  
251 area mixing ratio of ice-active mineral dust particles ( $=2.0 \times 10^{-6} \text{ m}^2\text{kg}^{-1}$ ) was considered in this  
252 study. Ice formation occurring below water saturation only was considered and, thus, Eqn. 1 in  
253 Phillips *et al.* (2008) was used for parameterizing ice nucleation.

254

### 255 2.3.1. SCAM5

256

257 Single column models are widely used to test physical parameterizations for use in the  
258 general circulation model (GCM). The model has 30 vertical levels, and the model time step is  
259 set to 10 min. The single column model resembles a single column of a GCM and can be derived  
260 from observations or model output. The complex feedbacks between the simulated column and  
261 other columns due to large-scale dynamics are not considered. Therefore, the single column  
262 model is an ideal tool for testing ice cloud parameterizations. The SCAM5 model was modified  
263 to incorporate the new parameterization developed in this study. The Barahona and Nenes (2008,  
264 2009a, b) scheme, which provides an analytical solution of the cloud parcel model equations  
265 (hereinafter called BN scheme), is used for calculating ice nucleation in cirrus clouds. The new  
266 AIDA  $n_s$ -isoline-based parameterizations as well as the P13 scheme were implemented in the  
267 model. The simulation was performed for one month (April 2010) at the United States  
268 Department of Energy's Atmospheric Radiation Measurement facility located at the SGP site  
269 (Hiranuma *et al.*, 2014).

270

### 271 2.3.2. COSMO

272

273 The non-hydrostatic weather forecast model, COSMO, was adapted to systematically  
274 investigate the impact of hematite particles under the simulated upper tropospheric conditions.

275 COSMO is the high-resolution limited-area model to assess clouds and convection at a  
276 horizontal spatial resolution of 2.8 km with 50 layers of stretched vertical grids. The time step is  
277 set to 20 seconds. In this study, we simulated a period of two days (July 23 to July 25, 2011) on a  
278 domain of 450 x 450 horizontal grid points centered over the German Alps (longitude: 0.1°E to  
279 18.7°E, latitude: 41.7°N to 53.2°N). The initial and boundary conditions were provided by the  
280 European Centre for Medium-Range Weather Forecasts. They are available at the  
281 Meteorological Archival and Retrieval System. In order to account for the spatio-temporal  
282 evolution of mass and number densities of six hydrometeor classes (i.e., cloud droplets,  
283 raindrops, cloud ice, snow, graupel and hail), the two-moment bulk microphysics scheme was  
284 incorporated in our COSMO model version following the method described by Seifert and  
285 Beheng (2006) and Seifert et al. (2012). Apart from the AIDA isoline-based freezing  
286 parameterization of hematite, two other ice nucleation modes, namely, M92 and homogeneous  
287 nucleation of cloud or solution droplets (Kärcher et al., 2006; Ren and MacKenzie, 2005), were  
288 considered in our COSMO simulations. The latter was used to parameterize the competition of  
289 water vapor between homogeneous and heterogeneous freezing.

290

## 291 3. Results

292

### 293 3.1. AIDA ice nucleation experiments

294

295 A series of AIDA experiments was carried out during the INUIT01 and INUIT04  
296 campaigns to investigate the ice nucleation efficiency of well-characterized hematite particles  
297 under water subsaturated conditions at  $-47\text{ }^{\circ}\text{C} < T$ . In addition, we used the AIDA results  
298 reported by Skrotzki *et al.* (2013) and reconciled them with the  $n_s$  values in order to parameterize  
299 the overall ice nucleation efficiency of hematite particles up to  $-78\text{ }^{\circ}\text{C}$ . In total, 12 expansion  
300 experiments, 4 from the INUIT campaigns and 8 from Skrotzki *et al.* (2013), were studied.  
301 Detailed experimental conditions and aerosol properties for these expansion experiments are  
302 summarized in Table 1. The use of different sizes of hematite particles in different temperature  
303 regions was justified by calculating the size-independent  $n_s$  values of 200 and 1000 nm diameter  
304 particles at  $\sim -40\text{ }^{\circ}\text{C}$ . For instance, the evaluated  $n_s$  values ( $10^{10}\text{ m}^{-2}$ ) for these two sizes agreed  
305 very well within  $\pm 1\%$   $\text{RH}_{\text{ice}}$  and  $\pm 0.3\text{ }^{\circ}\text{C}$  of chamber conditions (see corresponding  $\text{RH}_{\text{ice}}$  and  $T$   
306 at Evaluated  $n_s$  in Table 1 for INUIT04\_08, 1000 nm, HALO06\_19, 200 nm, and HALO06\_20,  
307 200 nm). This agreement verified the reproducibility of the AIDA chamber experiments, ice  
308 nucleation efficiency of hematite particles and size-independence of the  $n_s$  calculations. The  
309 advantage of using 1000 nm diameter hematite particles was that, due to their comparatively  
310 larger surface area, they were efficient in forming ice in cooling expansion experiments at  $-40$   
311  $^{\circ}\text{C} < T < -36\text{ }^{\circ}\text{C}$  (Hiranuma *et al.*, 2014).

312 The temporal profiles of deposition nucleation experiments from HALO campaigns,  
313 including  $N_{\text{ice}}$ , gas  $T$ ,  $\text{RH}_{\text{ice}}$  and  $\text{RH}_{\text{water}}$  measured by the TDL as well as the polarized light  
314 scattering properties in near-backscattering direction measured by SIMONE, are shown in Figure  
315 1. The depolarization ratio, which is sensitive to ice particle nucleation and growth, can be  
316 deduced from the latter. During a typical expansion, the air mass in the vessel experiences  
317 continuous cooling (for up to 500 s) and an increase in relative humidity (for up to 200 s, Fig. 1  
318 panel i and ii). Figure 1 panel iii shows the temporal plot of the depolarization ratio. At the  
319 beginning of the expansion, the depolarization ratio increases because ice is nucleating on the  
320 hematite particles. Conversely, repartitioning of gas phase water to ice phase water due to  
321 growing ice crystals triggers the declines in both depolarization ratio (i.e., sizing effect,

322 Schnaiter et al., 2012) and RH, usually after 100 s. The time-delay in our wet ice detection  
323 (typically 1  $\mu\text{m}$  is the minimum ice detection diameter for 200 and 500 nm diameter hematite  
324 particles) due to slower depositional growth after ice nucleation at lower  $T$  is accounted for in  
325 our error analyses (Figure 2). We evaluated only up to several hundred seconds of each  
326 expansion experiment as the ice nucleating period. Similar experimental profiles for INUIT  
327 campaigns are presented in Figure S1.

328 The initial  $n_s$ -isoline curves in the  $T$ -RH<sub>ice</sub> space are illustrated in Figure 2. Constant  $n_s$ -  
329 isoline curves are obtained by fitting second degree polynomial fit equations to the constant  $n_s$   
330 magnitudes calculated at various  $T$  and RH<sub>ice</sub> (see the supplement for more details). Previous  
331 AIDA results of two immersion freezing experiments (i.e., INUIT04\_13 and INUIT01\_28 from  
332 Hiranuma et al., 2014) are also shown on the water saturation line and used to constrain the  
333 fitted curves because immersion freezing is considered part of isolines. Since the  $n_s$  values  
334 presented in Fig. 3 of Hiranuma et al. (2014) only extends up to  $\sim 10^9 \text{ m}^{-2}$ , the data points of  
335 higher  $n_s$  values were extrapolated based on the observed values from two measurements. Figure  
336 2 shows several important features of  $n_s$ -isoline curves. First, below  $-60^\circ\text{C}$ ,  $n_s$ -isolines showed  
337 an increase in RH<sub>ice</sub> required to maintain a constant  $n_s$  (i.e.,  $n_s > 2.5 \times 10^8 \text{ m}^{-2}$ ) with decreasing  $T$   
338 (i.e., RH<sub>ice</sub>-dependent ice nucleation regime). For example, at a RH<sub>ice</sub> = 120% and  $T = -75^\circ\text{C}$ ,  
339 cooling by  $1^\circ\text{C}$  corresponds to a 10% decrease in  $n_s$ . This observation is interesting because the  
340 increase in RH<sub>ice</sub> required to maintain constant  $n_s$  values is consistent with the CNT for  
341 deposition nucleation (Eqn. A11 in Hoose and Möhler, 2012). Second, the highest sensitivity of  
342 RH<sub>ice</sub> is observed in a region where  $n_s$ -isolines are perpendicular to temperature-isolines ( $\sim -60^\circ\text{C}$   
343  $< T < \sim -50^\circ\text{C}$ ). Here,  $n_s$  is almost independent of  $T$ , and solely dependent on RH<sub>ice</sub>. Finally, we  
344 observed strong  $T$ -dependent nucleation near water saturation (i.e., while cooling along the water  
345 saturation line towards  $\sim -50^\circ\text{C}$ ). At a constant RH<sub>ice</sub> (e.g., 114%), for example, cooling by  $1^\circ\text{C}$   
346 from  $-41$  to  $-42^\circ\text{C}$  corresponds to an increase in  $n_s$  of approximately half an order of magnitude  
347 (see inset of Fig. 2). This suggests that the  $n_s$  values depend on temperature. Interestingly, we  
348 observed a continuous increase in  $n_s$  during cooling even after the depletion of supersaturation  
349 below  $-40^\circ\text{C}$  (Figure S2). CNT does not explain this predominant  $T$  contribution near water  
350 saturation (Fig. A1 in Hoose and Möhler, 2012). Therefore, other microphysical processes at the  
351 particle surface and/or perhaps even within the bulk phase may be responsible for this  $T$ -  
352 dependent behavior and these results appear to support the existence of a pore or surface freezing

353 process, as discussed in recent literature (e.g., Marcolli, 2014). In particular, we suspect that  
354 water condensation on the particle surface plays an important role on subsequent freezing. To  
355 support this, the surfaces of our hematite particles are not perfectly smooth and contain some  
356 active sites (e.g., pores and steps, Hiranuma et al., 2014). Moreover, water vapor may preferably  
357 fill the surface cavities due to the reduced saturation pressure in pores or at steps because of  
358 negative curvature Kelvin effects (Marcolli, 2014), thus leading to namely “surface condensation  
359 freezing (SCF)”. As described in previously published literatures (Christenson, 2013; Marcolli,  
360 2014), SCF may be of relevance to homogeneous nucleation (i.e., spontaneous ice nucleation in  
361 supercooled aerosol) at relevant  $T$  ( $< -36$  °C) and/or immersion mode freezing under water  
362 subsaturated conditions. Thus, SCF may arise from both homogeneous and heterogeneous  
363 nucleation.

364

### 365 3.2. Comparison with previous studies

366

367 The  $n_s$ -isolines of hematite particles were compared to previous measurements made  
368 using different aerosol species. This comparison was performed to (1) confirm that our  $n_s$  fit  
369 reproduces the overall trend shown by previous studies under certain  $T$ -RH<sub>ice</sub> conditions and (2)  
370 to demonstrate that the parameterization with laboratory-synthesized hematite particles  
371 quantitatively represents ice nucleation properties of atmospheric dust particles.

372 Comparison of the hematite  $n_s$ -isolines to previous deposition freezing observations are  
373 shown in Figure 3. More specifically, previous measurements were performed with natural  
374 Saharan desert dust (SD2, Möhler et al., 2006), reference Arizona test dust (ATD, Möhler et al.,  
375 2006; Welti et al., 2009), volcanic ash (Steinke et al., 2011), soot (Möhler et al., 2005), clay  
376 minerals (Welti et al., 2009; Koehler et al., 2010) and organics (Shilling et al., 2006; Wang and  
377 Knopf, 2011). These previous experimental studies used various types of ice nucleation  
378 instruments, such as substrate-supported cold stages coupled with an optical microscope (Shilling  
379 et al., 2006; Wang and Knopf, 2011), portable ice nuclei counters (Koehler et al., 2010; Welti et  
380 al., 2009) and the AIDA cloud simulation chamber (Möhler et al., 2005; Möhler et al., 2006;  
381 Steinke et al., 2011). They revealed the importance of both RH<sub>ice</sub> and temperature onto  
382 deposition mode ice nucleation of specific particle compositions. In Fig. 3a, previous AIDA  
383 results for dusts, ash and soot, are presented. Specifically, we utilized the  $T$ -RH<sub>ice</sub> data at  $\alpha =$



384 0.08 of SD2 and ATD reported in the previous AIDA study (Möhler *et al.*, 2006) to define  
385 isolines. It is noteworthy that an  $\alpha$  of 0.08 corresponds to  $\sim 10^{11} \text{ m}^{-2}$  in  $n_s$  when assuming  
386 uniform distributions of spherical particles of 0.5  $\mu\text{m}$  diameter ( $n_s = (-\ln(1-\alpha))/(\pi(0.5 \times 10^{-6})^2)$ ),  
387 which is in good agreement with the  $10^{11} \text{ m}^{-2}$   $n_s$ -isoline of hematite particles. For volcanic ash,  
388 we adapted  $n_s$  values ( $10^9$ ,  $5 \times 10^9$  and  $10^{10} \text{ m}^{-2}$ ) originally reported in Steinke *et al.*, (2011).  
389 Möhler *et al.* (2005) found that the ice nucleation of soot starts at the initial increase in polarized  
390 light scattering intensity in near-backscattering direction at 488 nm ( $n_s$  values are inaccessible).  
391 Except for these AIDA studies, other isolines in Fig. 3b and c were defined based on the reported  
392 ice nucleation measurements. For instance, Koehler *et al.* (2010) studied the deposition mode  
393 nucleation of size-selected (i.e., 200 nm, 300 nm, 400 nm) natural dusts, and reported ice  
394 nucleation conditions ( $T$  and  $\text{RH}_{\text{ice}}$ ) of ATD at  $\alpha = 0.01$  and of Canary Island Dust and Saharan  
395 Dust at  $\alpha = 0.05$ . Welti *et al.* (2009) also studied the deposition nucleation abilities of size-  
396 segregated mineral dusts (i.e., 100 to 800 nm diameter of ATD, illite, kaolinite and  
397 montmorillonite) based on  $\alpha = 0.01$ . Shilling *et al.* (2006) reported the ice nucleation onsets of  
398 ammonium sulfate and maleic acid detected by the decreasing partial pressure of water with  
399 FTIR-reflection absorption spectroscopy (e.g., 1 in  $10^5$  nucleation at about  $-33 \text{ }^\circ\text{C}$  for a spherical  
400 particle size of 1 to 10  $\mu\text{m}$  diameter). Wang and Knopf. (2011) investigated deposition freezing  
401 of various mineral and organic particles including kaolinite, Suwannee River standard fulvic acid  
402 and Leonardite standard humic acid particles. The authors reported the mean size of particles and  
403 associated ice-activated fractions at the given  $T$ - $\text{RH}_{\text{ice}}$ .

404 As seen in Fig. 3, the results from previous studies suggest the necessity of increasing  
405  $\text{RH}_{\text{ice}}$  to maintain a constant  $n_s$  value below  $T \sim -55^\circ\text{C}$ . They also indicate that nucleation may be  
406 triggered by SCF in the region where data and isolines approach water saturation where  
407 temperature plays a significant role on ice nucleation. It can also be observed that the contour of  
408 our new  $n_s$ -isoline parameterization of cubic hematite particles in  $T$ - $\text{RH}_{\text{ice}}$  coordinates generally  
409 agrees with the onsets determined by previous studies of other atmospherically relevant aerosols.  
410 In particular, the  $n_s$ -isolines estimated from ATD and SD2 ( $\sim 10^{11} \text{ m}^{-2}$ , Fig. 3a), which reasonably  
411 agree with the hematite  $n_s$ -isoline, suggest that atmospheric dust may have similar deposition  
412 mode ice nucleation efficiency.

413

### 414 3.3. $n_s$ -isoline-based parameterizations

415

416 Next, the ice nucleation efficiency of hematite particles was parameterized over a wide  
417 range of  $T$ - $RH_{ice}$ . Three types of parametrical descriptions used in this study are shown in Figure  
418 4. First, based on the AIDA experimental results, a series of constant  $n_s$  curves was interpolated  
419 to produce isolines in the range of  $10^6 \text{ m}^{-2} < n_s < 10^{12} \text{ m}^{-2}$  (Fig. 4a). The lower bound of  $n_s$  value  
420 ( $10^6 \text{ m}^{-2}$ ) was set based on the minimum  $n_s$  observed during AIDA expansions. Since the certain  
421 regions of  $n_s$ -isolines (i.e.,  $n_s < 7.5 \times 10^{10} \text{ m}^{-2}$ ; blue lines in Fig. 2) can submerge below ice  
422 saturation, the correction was applied to shift them and maintain all isolines above 100%  $RH_{ice}$ .  
423 The procedure to constrain  $n_s$  to  $>100\% RH_{ice}$  is described in the supplement (Fig. S3). Above  
424 the upper bound of  $10^{12} \text{ m}^{-2}$ ,  $n_s$  presumably remains constant up to the water saturation line in  
425 the  $T$ - $RH_{ice}$  space (no experimental data is available in this range). This assumption is valid in  
426 the present study because this  $n_s$  upper limit was hardly reached in our modeling case. However,  
427 more cloud simulation chamber measurements and data points for  $n_s \gg 10^{12} \text{ m}^{-2}$  are required to  
428 correctly constrain the  $n_s$  upper limit. It also has to be noted that the modeled ice crystal number  
429 concentration ( $\text{L}^{-1}$ ) derived from ice nucleation of hematite in this study is approximated by  
430 multiplying  $n_s$  by a simulated total surface of hematite ( $6.3 \times 10^{-10} \text{ m}^2 \text{ L}^{-1}$ ).

431 In the second fit approach (Fig. 4b), the interpolated  $n_s$  values were used to formulate the  
432  $n_s$ -isoline with a third degree-polynomial fit as a function of  $T$  ( $^{\circ}\text{C}$ ) and  $RH_{ice}$  (%) as

433

$$\begin{aligned} n_s^{3d}(T, RH_{ice}) = & -3.777 \times 10^{13} - 7.818 \times 10^{11} \cdot T + 4.252 \times 10^{11} \cdot RH_{ice} - 4.598 \\ & \times 10^9 \cdot T^2 + 6.952 \times 10^9 \cdot T \cdot RH_{ice} - 1.111 \times 10^9 \cdot RH_{ice}^2 - 2.966 \times 10^6 \cdot T^3 \\ & + 2.135 \times 10^7 \cdot T^2 \cdot RH_{ice} - 1.729 \times 10^7 \cdot T \cdot RH_{ice}^2 - 9.438 \times 10^5 \cdot RH_{ice}^3 \\ & \text{for } -78 \text{ }^{\circ}\text{C} < T < -36 \text{ }^{\circ}\text{C} \text{ and } 100 \% < RH_{ice} < \text{water saturation} \end{aligned} \quad (1)$$

434

435 where  $n_s^{3d}(T, RH_{ice})$  is the  $n_s$  derived from the third degree fit. The resulting spatial plot of  
436 isolines for constant  $n_s$  is shown in Fig. 4b. Note that the upper temperature boundary of  $-36 \text{ }^{\circ}\text{C}$   
437 was assigned as the interface between immersion mode- and deposition mode ice nucleation  
438 (*Hiranuma et al.*, 2014), and the lower boundary of  $-78 \text{ }^{\circ}\text{C}$  is the limit introduced by  
439 interpolating the hematite-isoline curves. The third approach (Fig. 4c) consisted in applying the  
440 equivalent  $n_s$  for deposition nucleation of hematite particles parameterized using the method  
441 introduced by *Phillips et al.* (2008 and 2013). In detail, we characterized the nucleation activity  
442

443 solely of mineral dust through the deposition mode by adapting the Equation (1) from *Phillips et*  
444 *al.* (2008), which accounts for nucleation under water subsaturated conditions, and excluded the  
445 contribution at water saturation, i.e., Equation (2) of *Phillips et al.* (2008). AIDA  $n_s$ -isoline-  
446 based parameterization suggests strong supersaturation dependence of  $n_s$  at low  $T$ . Observed  
447 diversity between a new parameterization (Figs. 4a and 4b) and P13 (Fig. 4c) may result in  
448 different ice crystal forming propensities and may predict different cloud properties. The  
449 potential consequence of observed diversity is demonstrated using conceptual models and  
450 discussed in the following section.

451

### 452 3.4. Model simulations

453

454 The SCAM5 results for monthly mean profiles of the simulated in-cloud  $N_{ice}$  ( $N_i \sim N_{ice}$ )  
455 over the ARM SGP site for five cases are shown in Figure 5. These include (Case 1) the pure  
456 homogeneous ice nucleation case, (Case 2-4) cases with contributions from both homogeneous  
457 and heterogeneous ice nucleation (hereinafter referred to as the combined case) described in Fig.  
458 4a-c (corresponding to Simulations A, B and C) and (Case 5) the simulation of the different  
459 lower boundaries of  $RH_{ice}$  ( $RH_i^*$ , Simulation D). In addition, the observed profile of ice crystal  
460 number concentrations is also shown in comparison to the simulations in Fig. 5. The  
461 observational data were collected over the SGP site on eight days of April 2010 during the Small  
462 PARTicles In Cirrus (SPARTICUS) campaign (*Zhang et al.*, 2013). The results of our  
463 simulations suggests that ice crystal formation due to heterogeneous ice nucleation processes  
464 inhibits homogeneous ice nucleation and significantly reduces the ice number concentrations for  
465 the AIDA parameterizations (Fig. 4a and b). In contrast, due to the much smaller ice crystal  
466 production from P13, as shown by the pure heterogeneous case in Figure 5, homogeneous ice  
467 nucleation in the P13 case (Fig. 4c) is less affected by heterogeneous nucleation. The observed  
468 mean profile of in-cloud ice crystal number concentrations is in agreement with the simulated  
469 ones. The differences between the three parameterizations derived from AIDA measurements,  
470 corresponding to Simulations A, B and D, are small for both the combined case and the pure  
471 heterogeneous ice nucleation case as presented in Fig. 6. This is because the BN scheme used in  
472 SCAM5 is based on parcel model theory and uses the predicted maximum ice supersaturation  
473 ( $S_{max}$ ) to calculate deposition ice nucleation rates.  $S_{max}$  is determined by assuming that the

474 supersaturation will reach its maximum where the depletion of water vapor compensates the  
475 supersaturation increase from cooling in a cloud parcel (i.e., BN scheme). The three  
476 parameterizations (i.e., Simulations A, B and D) have largest differences when  $RH_{ice}$  is below  
477 120% while  $S_{max}$  calculated in the model is often larger than 115%. This also explains the low  
478 sensitivity of  $N_{ice}$  to the lower bound of the onset  $RH_{ice}$  value (Figs. 5 and 6). We also  
479 investigated the impact of different particle size distributions on the calculation (not shown). The  
480 impact is small and negligible. The negligible sensitivity to the choice of AIDA  
481 parameterizations in SCAM5 simulations (Simulation A and B of Figs. 5 and 6) as well as the  
482 negligible sensitivity to the lower bound of the  $RH_{ice}$  value for ice nucleation,  $RH_i^*$  in Figs. 5 and  
483 6, reflect the limitation of SCAM5 as a large-scale model, which can't explicitly resolve the sub-  
484 grid (for the GCM grid box) variability of the supersaturation.

485 The results of the COSMO model for the vertical profiles of  $N_{ice}$  (presumably equivalent  
486 to the heterogeneous INP number concentration) are summarized in Figure 7. These results  
487 simulate the three different parameterization schemes (corresponding to Fig. 4a-c) in  
488 combination with homogeneous freezing.  $N_{ice}$  was spatially averaged over all areas of the model  
489 domain which in principle allow for deposition nucleation in our simulations, i.e. conditions  
490 below  $-36^\circ\text{C}$  and above 100%  $RH_{ice}$ . Because not always  $n_s$  is larger than zero (white areas of  
491 Fig. 2), also areas without ice formation are contained. It is also noteworthy that only purely  
492 heterogeneous ice formation is presented rather than the total ice occurring in the model. As  
493 shown in Fig. 7, the mean  $N_{ice}$  resulting from the parameterization based on P13 is smaller than  
494 that obtained from the AIDA  $n_s$ -isoline-based parameterization by more than two orders of  
495 magnitude. This large difference results predominantly from the inactivity of P13 at low  $RH_{ice}$ .  
496 Unlike the SCAM5 results, the COSMO results show the sensitivity to the different lower  
497 boundaries of  $RH_{ice}$  (i.e.,  $RH_i^* = 105\%$ , Simulation D). For instance, the mean  $N_{ice}$  below  $-36^\circ\text{C}$   
498 with a higher  $RH_{ice}$  boundary (105%) is reduced by 12%. This difference is perhaps due to the  
499 use of finely resolved grid-scale humidity in COSMO rather than parameterizing  $S_{max}$  as done in  
500 SCAM5 (Gettelman *et al.*, 2010). Figure 8 illustrates the differences between P13 and the AIDA  
501 results depending on  $T$  and  $RH_{ice}$ . Simulated  $N_{ice}$  values are segregated in fine  $T$  and  $RH_{ice}$   
502 spacing (1K and 2% bins, respectively) based on the thermodynamic conditions under which ice  
503 crystals were formed in COSMO and summed up over the time of simulation. This segregation  
504 allows for an estimation of the relative contribution of different thermodynamic conditions to the

505 simulated ice formation. Our results show diversity between P13 and the AIDA  $n_s$ -isoline-based  
506 parameterization. Ice crystal formation was less for P13 and more for the new parameterization.  
507 A possible explanation for the observed deviation may be due to the difference in  
508 parameterization based on lab- or field data. For instance, atmospheric aging and processing (i.e.,  
509 surface coating and associated heterogeneous surface reactions) may have altered ice-nucleating  
510 propensity and limited deposition nucleation of dust-derived INPs in the P13 parameterization  
511 for the field data-derived parameterization as discussed in *Phillips et al. (2008)*.

512

#### 513 4. Discussions

514

515 As described in the previous section (Sect. 3.1), deposition mode freezing cannot solely  
516 explain the  $n_s$ -isoline observation below water saturation ( $-50\text{ °C} < T < -36\text{ °C}$  in Fig. 2).

517 Although we presumed that SCF acts as a subset of immersion freezing and plays an important  
518 role in this region, further insight and evidence of SCF beyond cloud simulation chamber  
519 observations are required to correctly understand the contributions of both homogeneous and  
520 heterogeneous nucleation. High-resolution microscopic techniques with an integrated continuous  
521 cooling setup are needed to visualize the freezing process of a single particle and to fully  
522 understand the complex freezing processes involved in SCF on particle surfaces.

523 Comparison of the new parameterization to a previous empirical parameterization (P13)  
524 showed that the new AIDA  $n_s$ -isoline-based scheme predicts more ice (Figs. 4-8). In particular,  
525  $T$ -RH<sub>ice</sub> dependence of  $N_{ice}$  and  $n_s$  at low  $T$  that may coincide in the upper troposphere, and this  
526 highlights the need for further investigations. However, it should be noted that there is some  
527 evidence for the atmospheric relevance and applicability of the new parameterization. First of all  
528 we demonstrated that the new  $n_s$  parameterization based on the experiments with hematite  
529 particles agrees well with previous literature results for mineral dust aerosol (e.g., Möhler *et al.*,  
530 2006; Welti *et al.*, 2009; Köhler *et al.*, 2010). Second, Niemand *et al.* (2012) demonstrated that  
531 different dusts exhibit similar  $n_s$  in immersion mode freezing and perhaps such a similarity  
532 remains true for the deposition mode ice nucleation of desert dusts. Lastly, the comparison  
533 between the observed profile of ice crystal number concentrations and the simulated ones (Figs.  
534 5 and 6) also suggests the validity of the new parameterization. These premises must be further  
535 examined in comparing to atmospherically relevant substrates (fresh and aged ones) and their ice  
536 nucleation activities in laboratory settings. In situ INP measurements, such as the number  
537 concentration and the types of INPs, at the upper troposphere can also help to constrain the  
538 parameterization.

539 Finally, to further develop more atmospherically relevant parameterizations other than  
540 the fit-based parameterization with artificial test aerosol, the relationship between  $1/T$  and  $\ln S_{ice}$   
541 for a constant nucleation rate or  $n_s$  based on the CNT can be analyzed (i.e., Eqns. A10-A11 in  
542 Hoose and Möhler, 2012). In this way, the composition specific  $n_s(T-S_{ice})$  values, where the

543 transition from SCF to deposition nucleation (or vice versa) occurs, may be better defined and  
544 can be then be used as an inexpensive model friendly parameterization.

545

## 546 5. Conclusion

547

548 A new heterogeneous ice nucleation parameterization was developed using results  
549 obtained from AIDA cloud simulation chamber experiments. The new  $n_s$ -isoline-based  
550 parameterization is applicable to a wide temperature range from -36 to -78 °C and, hence, allows  
551 for the examination of ice nucleation spectra in a simple framework for modeling application.

552 Our experimental results provide a good basis for the  $T$  and  $RH_{ice}$  dependence of  
553 deposition nucleation, and the formulated hematite  $n_s$ -isolines are comparable to that of desert  
554 dust samples. Consequently, our results with synthesized hematite particles can also be relevant  
555 to cirrus applications despite their smaller atmospheric relevance compared to natural hematite.  
556 Our isoline formulation suggested three different ice nucleation pathways over the wide range of  
557 temperature. In specific, a  $RH_{ice}$ -dependent ice nucleation regime was observed at temperatures  
558 below  $\sim -60$  °C, where deposition mode is presumably responsible to trigger ice nucleation. At -  
559  $60$  °C  $< T < -50$  °C, ice nucleation efficiency was  $T$ -independent (i.e.,  $RH_{ice}$  dependent).  
560 Conversely, a predominant influence of  $T$  on ice nucleation was observed near the water  
561 saturation condition ( $T > \sim -50$  °C), which may be indicative of nucleation due to condensation of  
562 water at the particle surface followed by homogeneous freezing of the condensed water (i.e.,  
563 SCF). The observed active SCF near water saturation and physical processes at the transitions of  
564 nucleation modes still remain to be studied in detail for various types of atmospheric particles.

565 Our conceptual model examinations also considered the competition between  
566 heterogeneous freezing and homogeneous freezing of solution particles to evaluate the relative  
567 importance of the different freezing processes in two models (SCAM5 and COSMO). The  
568 inhibition of homogeneous nucleation due to heterogeneous freezing was commonly observed in  
569 both SCAM5 and COSMO simulations. Our new parameterization revealed a minimum  
570 deviation of  $N_{ice}$  values estimated by SCAM5 at minimum  $RH_{ice}$  values for ice formation (100 or  
571 105%) compared to COSMO. This deviation suggests different sensitivities of the model to the  
572 lower bound of the  $RH_{ice}$  value owing to the presence of the model-resolved supersaturation to  
573 calculate the ice nucleation rate. Overall, our new hematite-based parameterization strongly  
574 suggests the role of  $T$  and more ice nucleation when compared to the existing empirical  
575 parameterization, presumably allowing more ice activation under water subsaturated conditions.

576



577 **Author Contributions**

578

579 N. Hiranuma and O. Möhler designed and conceived the experiments. Parameterizations  
580 were implemented by N. Hiranuma, I. Steinke and M. Paukert. M. Paukert and K. Zhang carried  
581 out modeling studies with input from C. Hoose, N. Hiranuma and G. Kulkarni. M. Schnaiter  
582 analyzed SIMONE data. H. Saathiff contributed to TDL measurements and analysis. The  
583 manuscript was written by N. Hiranuma. All authors discussed the results and contributed ideas  
584 to the manuscript.

585

586 **Acknowledgements**

587

588 This work was supported by the German Research Foundation (Deutsche  
589 Forschungsgemeinschaft, DfG) under contracts MO 668/4-1 and HO 4612/1-1 within the  
590 Research Unit FOR 1525 (INUIT) and by the Helmholtz Association's research programme  
591 "Atmosphere and Climate (ATMO)". The authors acknowledge partial financial support by DfG  
592 and Open Access Publishing Fund of Karlsruhe Institute of Technology. K. Zhang and G.  
593 Kulkarni acknowledge support from the Department of Energy Atmospheric System Research  
594 Program. The Pacific Northwest National Laboratory is operated for DOE by Battelle Memorial  
595 Institute under contract DE-AC05-76RLO 1830. We would like to thank R. Buschbacher, T.  
596 Chudy, E. Kranz, G. Scheurig and S. Vogt for their professional support for the AIDA chamber  
597 operation during the INUIT campaigns. We also thank P. Weidler and S. Jaeger for support in  
598 preparing the hematite particles. M. Hummel's contribution to the model setup is gratefully  
599 acknowledged.

600

601 **References**

602  
603  
604  
605  
606  
607  
608  
609  
610  
611  
612  
613  
614  
615  
616  
617  
618  
619  
620  
621  
622  
623  
624  
625  
626  
627  
628  
629  
630  
631  
632  
633  
634  
635  
636  
637  
638  
639  
640  
641  
642  
643  
644  
645

Archuleta, C. M., DeMott, P. J., and Kreidenweis, S. M.: Ice nucleation by surrogates for atmospheric mineral dust and mineral dust/sulfate particles at cirrus temperatures, *Atmos. Chem. Phys.*, 5, 2617–2634, doi:10.5194/acp-5-2617-2005, 2005.

Baldauf, M., Seifert, A., Förstner, J., Majewski, D., Raschendorfer, M., and Reinhardt, T.: Operational convective-scale numerical weather prediction with the COSMO model: Description and sensitivities, *Mon. Weather Rev.*, 139, 12, 3887–3905, doi: 10.1175/MWR-D-10-05013.1, 2011.

Barahona, D. and Nenes, A.: Parameterization of cirrus cloud formation in large-scale models: Homogeneous nucleation, *J. Geophys. Res.*, 113, D11211, doi:10.1029/2007JD009355, 2008.

Barahona, D. and Nenes, A.: Parameterizing the competition between homogeneous and heterogeneous freezing in cirrus cloud formation – monodisperse ice nuclei, *Atmos. Chem. Phys.*, 9, 369–381, doi:10.5194/acp-9-369-2009, 2009a.

Barahona, D. and Nenes, A.: Parameterizing the competition between homogeneous and heterogeneous freezing in ice cloud formation – polydisperse ice nuclei, *Atmos. Chem. Phys.*, 9, 5933–5948, doi:10.5194/acp-9-5933-2009, 2009b.

Barahona, D., Rodriguez, J., and Nenes, A.: Sensitivity of the global distribution of cirrus ice crystal concentration to heterogeneous freezing, *J. Geophys. Res.*, 115, D23213, doi:10.1029/2010JD014273, 2010.

Benz, S., Megahed, K., Möhler, O., Saathoff, H., Wagner, R., and Schurath, U.: *T*-dependent rate measurements of homogeneous ice nucleation in cloud droplets using a large atmospheric simulation chamber, *J. Photoch. Photobio. A*, 176, 208–217, doi:10.1016/j.jphotochem.2005.08.026, 2005.

Boucher, O., Randall, D., Artaxo, P., Bretherton, C., Feingold, G., Forster, P., Kerminen, V.-M., Kondo, Y., Liao, H., Lohmann, U., Rasch, P., Satheesh, S. K., Sherwood, S., Stevens, B., and Zhang, X. Y.: Clouds and Aerosols. In: *Climate Change 2013: The Physical Science Basis. Contribution of Working Group I to the Fifth Assessment Report of the Intergovernmental Panel on Climate Change* [Stocker, T. F., D. Qin, G.-K. Plattner, M. Tignor, S. K. Allen, J. Boschung, A. Nauels, Y. Xia, V. Bex, and P. M. Midgley (eds.)]. Cambridge University Press, Cambridge, United Kingdom and New York, NY, USA, 2013.

Christenson, H.: Two-step crystal nucleation via capillary condensation, *Cryst. Eng. Comm.*, 15, 2030–2039, doi:10.1039/C3CE26887J, 2013.

Claquin, T., Schulz, M., and Balkanski, Y.: Modeling the mineralogy of atmospheric dust sources, *J. Geophys. Res.*, 104, 22243–22256, doi:10.1029/1999JD900416, 1999.

646 Connolly, P.J., Möhler, O., Field, P.R., Saathoff, H., Burgess, R., Choullarton, T., and Gallagher,  
647 M.: Studies of heterogeneous freezing by three different desert dust samples, *Atmos. Chem.*  
648 *Phys.*, 9, 2805–2824, doi:10.5194/acp-9-2805-2009, 2009.

649

650 Cziczo, D. J., Froyd, K. D., Hoose, C., Jensen, E. J., Diao, M., Zondlo, M. A., Smith J. B.,  
651 Twohy, C. H., and Murphy, D. M.: Clarifying the dominant sources and mechanisms of cirrus  
652 cloud formation, *Science*, 340, 1320–1324, doi:10.1126/science.1234145, 2013.

653

654 Cziczo, D. J. and Froyd, K. D.: Sampling the composition of cirrus ice residuals, *Atmospheric*  
655 *Research*, 142, 15–31, doi: 10.1016/j.atmosres.2013.06.012, 2014.

656

657 DeMott, P. J., Möhler, O., Stetzer, O., Vali, G., Levin, Z., Petters, M. D., Murakami, M., Leisner,  
658 T., Bundke, U., Klein, H., Kanji, Z. A., Cotton, R., Jones, H., Benz, S., Brinkmann, M.,  
659 Rzesanke, D., Saathoff, H., Nicolet, M., Saito, A., Nillius, B., Bingemer, H., Abbatt, J., Ardon,  
660 K., Ganor, E., Georgakopoulos, D. G., and Saunders, C.: **Resurgence in ice nuclei**  
661 **measurement research**, *Bulletin of the Amer. Meteorol. Soc.*, 92, 1623–1625,  
662 doi:http://dx.doi.org/10.1175/2011BAMS3119.1, 2011.

663

664 Doms, G., Förster, J., Heise, E., Herzog, H.-J., Mironov, D., Raschendorfer, M., Reinhardt, T.,  
665 Ritter, B., Schrodin, R., Schulz, J.-P., and Vogel, G.: A description of the nonhydrostatic  
666 regional COSMO Model. Part II: Physical parameterization, Technical Report. Deutscher  
667 Wetterdienst, 154 pp, 2011.

668

669 Fahey, D. W., Gao, R.-S., Möhler, O., Saathoff, H., Schiller, C., Ebert, V., Krämer, M., Peter, T.,  
670 Amarouche, N., Avallone, L. M., Bauer, R., Bozóki, Z., Christensen, L. E., Davis, S. M.,  
671 Durr, G., Dyroff, C., Herman, R. L., Hunsmann, S., Khaykin, S. M., Mackrodt, P., Meyer, J.,  
672 Smith, J. B., Spelten, N., Troy, R. F., Vömel, H., Wagner, S., and Wienhold, F. G.: The  
673 AquaVIT-1 intercomparison of atmospheric water vapor measurement techniques, *Atmos. Meas.*  
674 *Tech. Discuss.*, 7, 3159–3251, doi:10.5194/amtd-7-3159-2014, 2014.

675

676 Gettelman, A., Hegglin, M. I., Son, S.-W., Kim, J., Fujiwara, M., Birner, T., Kremser, S., Rex,  
677 M., Añel, J. A., Akiyoshi, H., Austin, J., Bekki, S., Braesike, P., Brühl, C., Butchart, N.,  
678 Chipperfield, M., Dameris, M., Dhomse, S., Garny, H., Hardiman, S. C., Jöckel, P., Kinnison, D.  
679 E., Lamarque, J. F., Mancini, E., Marchand, M., Michou, M., Morgenstern, O., Pawson, S., Pitari,  
680 G., Plummer, D., Pyle, J.A., Rozanov, E., Scinocca, J., Shepherd, T. G., Shibata, K., Smale, D.,  
681 Teyssèdre, H., and Tian, W.: Multimodel assessment of the upper troposphere and lower  
682 stratosphere: Tropics and global trends, *J. Geophys. Res.*, 115, D00M08,  
683 doi:10.1029/2009JD013638, 2010.

684

685 Hiranuma, N., Hoffmann, N., Kiselev, A., Dreyer, A., Zhang, K., Kulkarni, G., Koop, T., and  
686 Möhler, O.: Influence of surface morphology on the immersion mode ice nucleation efficiency of  
687 hematite particles, *Atmos. Chem. Phys.*, 14, 2315–2324, doi:10.5194/acp-14-2315-2014, 2014.

688

689 Hoose, C., Kristjánsson, J.E., Chen, J.-P., and Hazra, A.: A classical-theory-based  
690 parameterization of heterogeneous ice nucleation by mineral dust, soot and biological particles in

691 a global climate model, *J. Atmos. Sci.*, 67(8) 2483–2503,  
692 doi:<http://dx.doi.org/10.1175/2010JAS3425.1>, 2010.  
693  
694 Hoose, C and Möhler, O.: Heterogeneous ice nucleation on atmospheric aerosols: a review of  
695 results from laboratory experiments, *Atmos. Chem. Phys.*, 12, 9817–9854,  
696 doi:10.5194/acp-12-9817-2012, 2012.  
697  
698 Hung H.-M., Malinowski, A., and Martin, S. T.: Kinetics of heterogeneous ice nucleation on the  
699 surfaces of mineral dust cores inserted into aqueous ammonium sulfate particles, *J. Phys. Chem.*  
700 *A.*, 107, 1296–1306, doi: 10.1021/jp021593y, 2003.  
701  
702 Kärcher, B. and Lohmann, U.: A parameterization of cirrus cloud formation: Heterogeneous  
703 freezing, *J. Geophys. Res.*, 108, 4402, doi:10.1029/2002JD003220, 2003.  
704  
705 Kärcher, B., Hendricks, J., and Lohmann, U.: Physically based parameterization of cirrus cloud  
706 formation for use in global atmospheric models, *J. Geophys. Res.*, 111, D01, 205,  
707 doi:10.1029/2005JD006219, 2006.  
708  
709 Khvorostyanov, V. I. and Curry, J. A.: The theory of ice nucleation by heterogeneous freezing of  
710 deliquescent mixed CCN. Part I: Critical radius, energy, and nucleation rate, *J. Atmos. Sci.*, 61,  
711 2676–2691, doi:<http://dx.doi.org/10.1175/JAS3266.1>, 2004.  
712  
713 Koehler, K. A., Kreidenweis, S. M., DeMott, P. J., Petters, M. D., Prenni, A. J., and Möhler, O.:  
714 Laboratory investigations of the impact of mineral dust aerosol on cold cloud formation, *Atmos.*  
715 *Chem. Phys.*, 10, 11955–11968, doi:10.5194/acp-10-11955-2010, 2010.  
716  
717 Koop, T., Luo, B., Tsias, A., and Peter, T.: Water activity as the determinant for homogeneous  
718 ice nucleation in aqueous solutions, *Nature*, 406, 611–614, doi:10.1038/35020537, 2000.  
719  
720 Liu, X. and Penner, J. E.: Ice nucleation parameterization for global models, *Meteorol. Z.*, 14,  
721 499–514, doi:10.1127/0941-2948/2005/0059, 2005.  
722  
723 Liu, X., Shi, X., Zhang, K., Jensen, E. J., Gettelman, A., Barahona, D., Nenes, A., and Lawson,  
724 P.: Sensitivity studies of dust ice nuclei effect on cirrus clouds with the Community Atmosphere  
725 Model CAM5, *Atmos. Chem. Phys.*, 12, 12061–12079, doi:10.5194/acp-12-12061-2012, 2012.  
726  
727 Marcolli, C.: Deposition nucleation viewed as homogeneous or immersion freezing in pores and  
728 cavities, *Atmos. Chem. Phys.*, 14, 2071–2104, doi:10.5194/acp-14-2071-2014, 2014.  
729  
730 Matsuki, A., Schwarzenboeck, A., Venzac, H., Laj, P., Crumeyrolle, S., and Gomes, L.: Cloud  
731 processing of mineral dust: direct comparison of cloud residual and clear sky particles during  
732 AMMA aircraft campaign in summer 2006, *Atmos. Chem. Phys.*, 10, 1057–1069,  
733 doi:10.5194/acp-10-1057-2010, 2010.  
734

735 Meyers, M. P., DeMott, P. J., and Cotton, W. R.: New primary ice nucleation parameterizations  
736 in an explicit cloud model, *J. Appl. Meteorol.*, 31, 708–721, doi:[http://dx.doi.org/10.1175/1520-0450\(1992\)031<0708:NPINPI>2.0.CO;2](http://dx.doi.org/10.1175/1520-0450(1992)031<0708:NPINPI>2.0.CO;2), 1992.

737  
738

739 Möhler, O., Stetzer, O., Schaefers, S., Linke, C., Schnaiter, M., Tiede, R., Saathoff, H., Krämer,  
740 M., Mangold, A., Budz, P., Zink, P., Schreiner, J., Mauersberger, K., Haag, W., Kärcher, B., and  
741 Schurath, U.: Experimental investigation of homogeneous freezing of sulphuric acid particles in  
742 the aerosol chamber AIDA, *Atmos. Chem. Phys.*, 3, 211–223, doi:10.5194/acp-3-211-2003,  
743 2003.

744

745 Möhler, O., Linke, C., Saathoff, H., Schnaiter, M., Wagner, R., Mangold, A., Krämer, M., and  
746 Schurath, U.: Ice nucleation on flame soot aerosol of different organic carbon content, *Meteorol.*  
747 *Z.*, 14, 477–484, doi:10.1127/0941-2948/2005/0055, 2005.

748

749 Möhler, O., Field, P. R., Connolly, P., Benz, S., Saathoff, H., Schnaiter, M., Wagner, R., Cotton,  
750 R., Krämer, M., Mangold, A., and Heymsfield, A. J.: Efficiency of the deposition mode ice  
751 nucleation on mineral dust particles, *Atmos. Chem. Phys.*, 6, 3007–3021, doi:10.5194/acp-6-  
752 3007-2006, 2006.

753

754 Murray, B. J., O’Sullivan, D., Atkinson, J. D., and Webb, M. E.: Ice nucleation by particles  
755 immersed in supercooled cloud droplets, *Chem. Soc. Rev.*, **41**, 6519–6554,  
756 doi:10.1039/c2cs35200a, 2012.

757

758 Neale, R. B., Chen, C.-C., Gettelman, A., Lauritzen, P. H., Park, S., Williamson, D. L., Conley,  
759 A. J., Garcia, R., Kinnison, D., Lamarque, J.-F., Marsh, D., Mills, M., Smith, A. K., Tilmes, S.,  
760 Vitt, F., Morrison, H., Cameron-Smith, P., Collins, W. D., Iacono, M. J., Easter, R. C., Ghan, S.  
761 J., Liu, X., Rasch, P. J., and Taylor, M. A.: Description of the NCAR Community At- mosphere  
762 Model (CAM5.0), Tech. Rep. NCAR/TN-486-STR, NCAR, available at:  
763 <http://www.cesm.ucar.edu/models/cesm1.0/cam/> (last access: 8 January 2013), 2010.

764

765 Niemand, M., Möhler, O., Vogel, B., Vogel, H., Hoose, C., Connolly, P., Klein, H., Bingemer,  
766 H., DeMott, P., Skrotzki, J., and Leisner, T.: A particle-surface-area-based parameterization of  
767 immersion freezing on mineral dust particles, *J. Atmos. Sci.*, 69, 3077–3092,  
768 doi:<http://dx.doi.org/10.1175/JAS-D-11-0249.1>, 2012.

769

770 Phillips, V. T. J., DeMott, P. J., and Andronache, C.: An empirical parameterization of  
771 heterogeneous ice nucleation for multiple chemical species of aerosol, *J. Atmos. Sci.*, 65, 2757–  
772 2783, doi:<http://dx.doi.org/10.1175/2007JAS2546.1>, 2008.

773

774 Phillips, V. T. J., DeMott, P. J., Andronache, C., Pratt, K. A., Prather, K. A., Subramanian, R.,  
775 and Twohy, C.: Improvements to an empirical parameterization of heterogeneous ice nucleation  
776 and its comparison with observations, *J. Atmos. Sci.*, 70, 378–409, doi:  
777 <http://dx.doi.org/10.1175/JAS-D-12-080.1>, 2013.

778

779 Pruppacher, H. R. and Klett, J. D.: Microphysics of Clouds and Precipitation, Atmospheric and  
780 Oceanographic Sciences Library, Kluwer Academic Publishers, Dordrecht, The Netherlands,  
781 309–360, 1997.  
782  
783 Ren, C. and Mackenzie, A. R.: Cirrus parameterization and the role of ice nuclei, *Q. J. Roy.*  
784 *Meteorol. Soc.*, 131, 1585–1605, doi:10.1256/qj.04.126, 2005.  
785  
786 Sakai, T., Orikasa, N., Nagai, T., Murakami, M., Tajiri, T., Saito, A., Yamashita, K., and  
787 Hashimoto, A.: Balloon-borne and Raman lidar observations of Asian dust and cirrus cloud  
788 properties over Tsukuba, Japan, *J. Geophys. Res.*, 119, 3295–3308, doi:10.1002/2013JD020987,  
789 2014.  
790  
791 Sassen, K. and Khvorostyanov, V. I.: Cloud effects from boreal forest fire smoke: Evidence for  
792 ice nucleation from polarization lidar data and cloud model simulations, *Environ. Res. Lett.*, 3,  
793 025006, doi:10.1088/1748-9326/3/2/025006, 2008.  
794  
795 Schnaiter, M., Büttner, S., Möhler, O., Skrotzki, J., Vragel, M., and Wagner, R.: Influence of  
796 particle size and shape on the backscattering linear depolarisation ratio of small ice crystals –  
797 cloud chamber measurements in the context of contrail and cirrus microphysics, *Atmos. Chem.*  
798 *Phys.*, 12, 10465–10484, doi:10.5194/acp-12-10465-2012, 2012.  
799  
800 Seifert, A. and Beheng, K. D.: A two-moment cloud microphysics parameterization for mixed-  
801 phase clouds. Part I: Model description, *Meteorol. Atmos. Phys.*, 92, 45–66, doi:10.1007/s00703-  
802 005-0112-4, 2006.  
803  
804 Seifert, A., Köhler, C., and Beheng, K. D.: Aerosol-cloud-precipitation effects over Germany as  
805 simulated by a convective-scale numerical weather prediction model, *Atmos. Chem. Phys.*, 12  
806 (2), 709–725, doi:10.5194/acp-12-709-2012, 2012.  
807  
808 Shilling, J. E., Fortin, T. J., and Tolbert, M. A.: Depositional ice nucleation on crystalline organic  
809 and inorganic solids, *J. Geophys. Res.*, 111, D05207, doi:10.1029/2005JD006664, 2006.  
810  
811 Skrotzki, J., Connolly, P., Schnaiter, M., Saathoff, H., Möhler, O., Wagner, R., Niemand, M.,  
812 Ebert, V., and Leisner, T.: The accommodation coefficient of water molecules on ice – cirrus  
813 cloud studies at the AIDA simulation chamber, *Atmos. Chem. Phys.*, 13, 4451–4466,  
814 doi:10.5194/acp-13-4451-2013, 2013.  
815  
816 Steinke, I., Möhler, O., Kiselev, A., Niemand, M., Saathoff, H., Schnaiter, M., Skrotzki, J.,  
817 Hoose, C., and Leisner, T.: Ice nucleation properties of fine ash particles from the  
818 Eyjafjallajökull eruption in April 2010, *Atmos. Chem. Phys.*, 11, 12945–12958, doi:10.5194/acp-  
819 11-12945-2011, 2011.  
820  
821 Storelvmo, T. and Herger, N.: Cirrus cloud susceptibility to the injection of ice nuclei in the  
822 upper troposphere, *J. Geophys. Res.*, 119, 2375–2389, doi:10.1002/2013JD020816, 2014.  
823

824 Sugimoto, T. and Sakata, K.: Preparation of monodisperse pseudocubic  $\alpha$ -Fe<sub>2</sub>O<sub>3</sub> particles from  
825 condensed ferric hydroxide gel, **J. Colloid Interface Sci.**, 152, 2, 587–590, doi:10.1016/0021-  
826 9797(92)90062-Q, 1992.

827

828 Vali, G.: Nucleation terminology, **J. Aerosol Sci.**, 16, 575–576, doi:10.1016/0021-  
829 8502(85)90009-6, 1985.

830

831 Vragel, M.: Messung klimarelevanter optischer Eigenschaften von Mineralstaub im Labor,  
832 Faculty of Physics, Karlsruhe Institute of Technology, Karlsruhe, 162 pp., 2009.

833

834 Wang, B. and Knopf, D.: Heterogeneous ice nucleation on particles composed of humic-like  
835 substances impacted by O<sub>3</sub>, **J. Geophys. Res.**, 116, D03205, doi:10.1029/2010JD014964, 2011.

836

837 Welti, A., Lüönd, F., Stetzer, O., and Lohmann, U.: Influence of particle size on the ice  
838 nucleating ability of mineral dusts, **Atmos. Chem. Phys.**, 9, 6705–6715, doi:10.5194/acp-9-6705-  
839 2009, 2009.

840

841 Welti, A., Kanji, Z. A., Lüönd, F., Stetzer, O., and Lohmann, U.: Exploring the mechanisms of  
842 ice nucleation on kaolinite: from deposition nucleation to condensation freezing, **J. Atmos. Sci.**,  
843 71, 16–36, doi: 10.1175/JAS-D-12-0252.1, 2014.

844

845 Zhang, K., Liu, X., Wang, M., Comstock, J. M., Mitchell, D. L., Mishra, S., and Mace, G. G.:  
846 Evaluating and constraining ice cloud parameterizations in CAM5 using aircraft measurements  
847 from the SPARTICUS campaign, **Atmos. Chem. Phys.**, 13, 4963–4982, doi:10.5194/acp-13-  
848 4963-2013, 2013.

849

850 Zuberi, B., Bertram, A. K., Cassa, C. A., Molina, L. T., and Molina, M. J.: Heterogeneous  
851 nucleation of ice in (NH<sub>4</sub>)<sub>2</sub>SO<sub>4</sub>–H<sub>2</sub>O particles with mineral dust immersions, **Geophys. Res.**  
852 **Let.**, 29, 1504, doi:10.1029/2001GL014289, 2002.

853



854 **Table and Figures of “A Comprehensive Parameterization of Heterogeneous Ice Nucleation**  
855 **of Dust Surrogate: Laboratory study with Hematite Particles and Its Application to**  
856 **Atmospheric Models”**  
857

858 **October 1, 2014**

859

860

861 Naruki Hiranuma<sup>a,\*</sup>, Marco Paukert<sup>a</sup>, Isabelle Steinke<sup>a</sup>, Kai Zhang<sup>b</sup>, Gourihar Kulkarni<sup>b</sup>,  
862 Corinna Hoose<sup>a</sup>, Martin Schnaiter<sup>a</sup>, Harald Saathoff<sup>a</sup> and Ottmar Möhler<sup>a</sup>

863

864

865 <sup>a</sup>*Institute for Meteorology and Climate Research – Atmospheric Aerosol Research,*  
866 *Karlsruhe Institute of Technology, Karlsruhe, Germany.*

867 <sup>b</sup>*Atmospheric Science and Global Change Division,*

868 *Pacific Northwest National Laboratory, Richland, Washington, USA*

869

870

871 \*Corresponding Author. E-mail: seong.moon@kit.edu

872

873

874

875

876

877

878

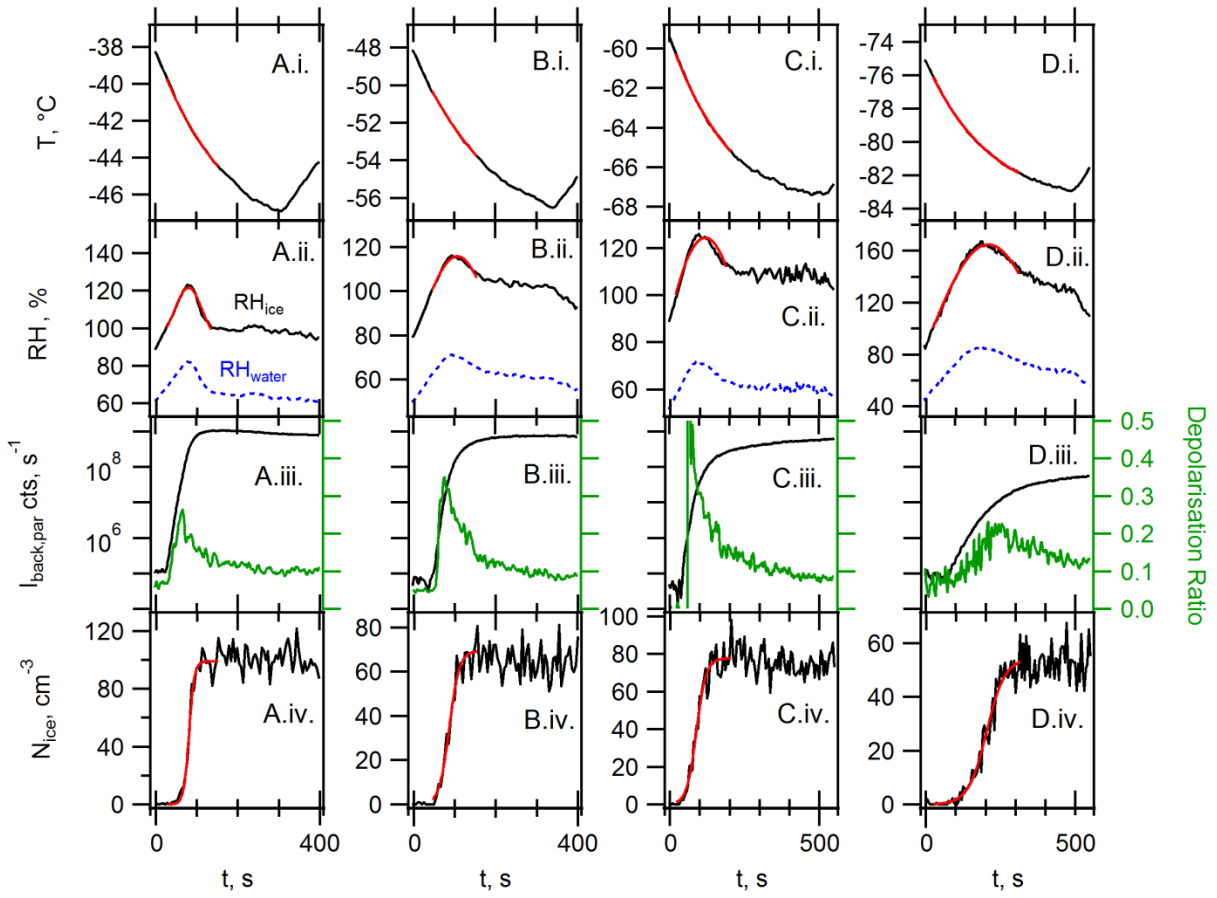
879 **Citation:**

880 Hiranuma, N. et al. **A Comprehensive Parameterization of Heterogeneous Ice Nucleation of**  
881 **Dust Surrogate: Laboratory study with Hematite Particles and Its Application to**  
882 **Atmospheric Models**, for *Atmospheric Chemistry and Physics*

Table 1. Summary of aerosol measurements and AIDA ice nucleation experiments. All HALO experiments are from Skrotzki *et al.* (2013).

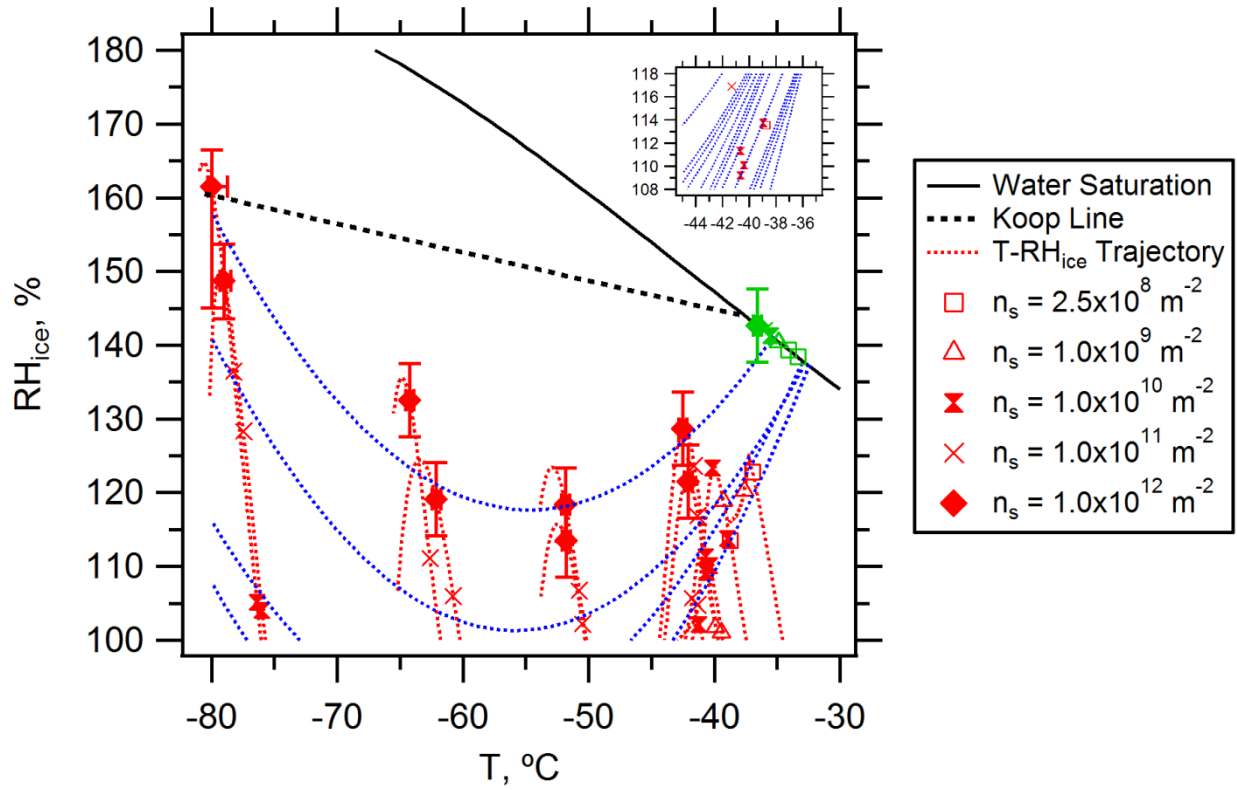
Experiment ID	Aerosol Measurements			Ice Nucleation Measurements				
	Hematite Diameter, nm	Total Number Conc., cm <sup>-3</sup>	Total Surface Conc., μm <sup>2</sup> cm <sup>-3</sup>	Examined <i>T</i> Range, °C	Examined RH <sub>ice</sub> Range, %	Evaluated <i>n<sub>s</sub></i> , m <sup>-2</sup>	<i>T</i> (Evaluated <i>n<sub>s</sub></i> ), °C	RH <sub>ice</sub> (Evaluated <i>n<sub>s</sub></i> ), %
HALO05_24	200	115.0	14.4	-76.1 to -81.9	100.6 to 164.8	10 <sup>11</sup>	-78.2	136.4
HALO04_09	500	112.5	26.9	-75.8 to -80.1	100.3 to 149.8	10 <sup>11</sup>	-77.5	128.3
HALO04_05	500	142.2	30.9	-61.8 to -65.5	100.2 to 135.6	10 <sup>11</sup>	-62.6	111.1
HALO05_18	200	161.9	21.8	-60.3 to -65.2	100.1 to 124.5	10 <sup>11</sup>	-60.8	106.0
HALO06_22	200	145.7	19.2	-50.2 to -53.9	100.3 to 123.4	10 <sup>11</sup>	-50.7	106.7
HALO06_21	200	245.0	32.9	-50.3 to -53.8	100.4 to 115.8	10 <sup>11</sup>	-50.5	102.2
INUIT01_26	1000	342.1	749.0	-41.0 to -47.1	100.2 to 103.9	10 <sup>10</sup>	-41.2	102.2
HALO06_20	200	168.7	22.4	-39.8 to -44.4	100.4 to 128.8	10 <sup>10</sup>	-40.7	111.3
HALO06_19	200	283.0	42.9	-39.7 to -44.5	100.2 to 121.6	10 <sup>10</sup>	-40.6	109.2
INUIT04_08	1000	193.0	647.0	-39.3 to -45.4	100.0 to 113.2	10 <sup>10</sup>	-40.4	110.1
INUIT04_10	1000	161.7	546.6	-37.5 to -43.7	100.0 to 124.1	10 <sup>10</sup>	-40.1	123.3
INUIT01_30	1000	414.5	889.7	-34.6 to -42.0	100.2 to 127.1	2.5 x 10 <sup>8</sup>	-37.0	122.8

883  
884



885  
886

Figure 1.



887  
888  
889

Figure 2.

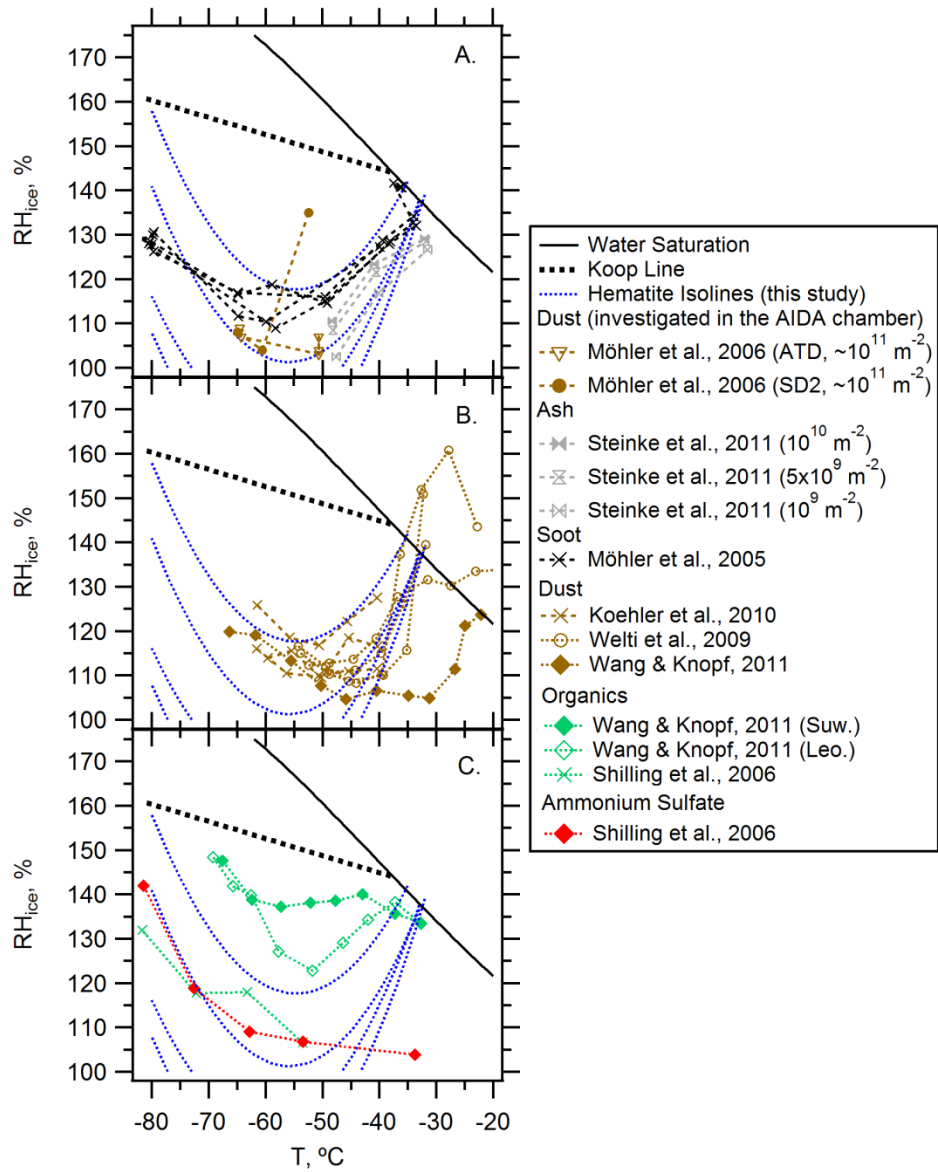
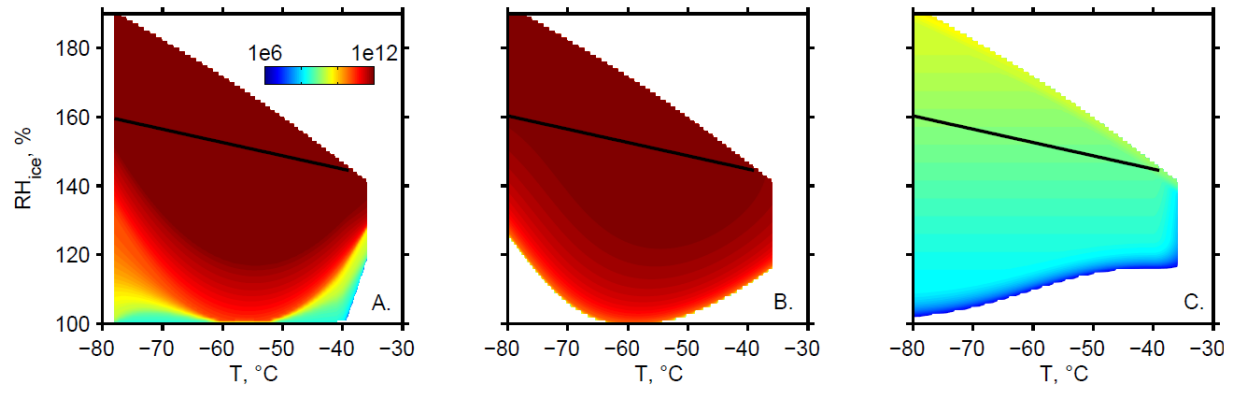


Figure 3.

890  
891  
892

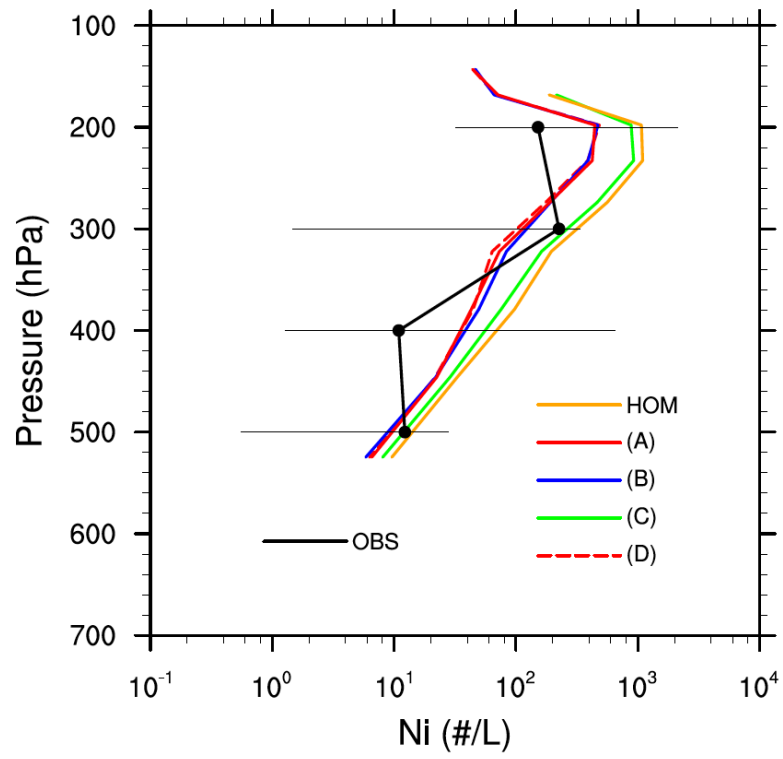
893



894  
895  
896

Figure 4.

897

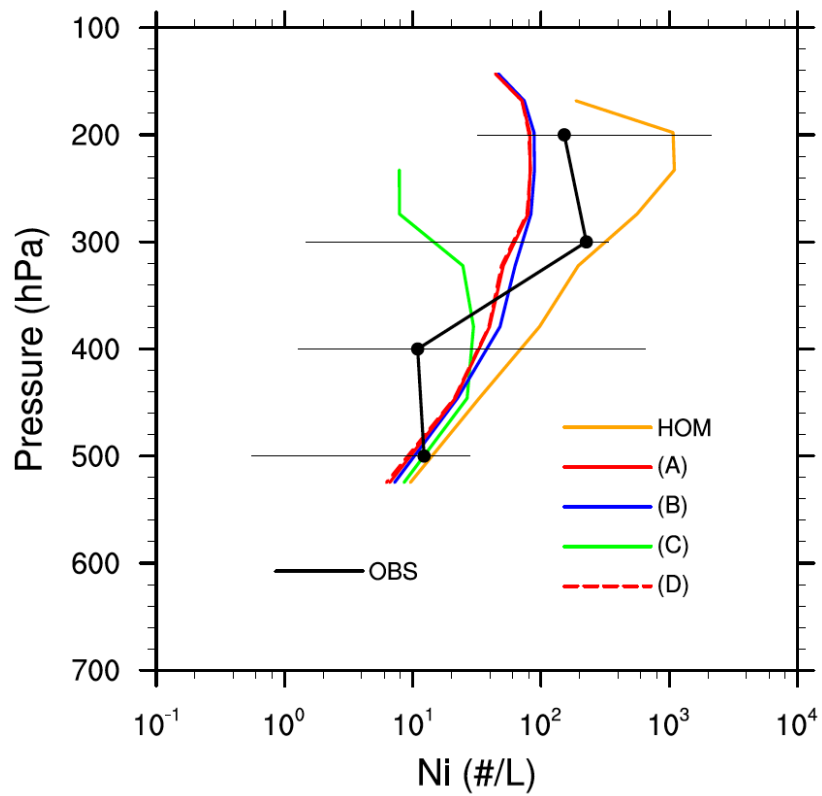


898

899

Figure 5.

900



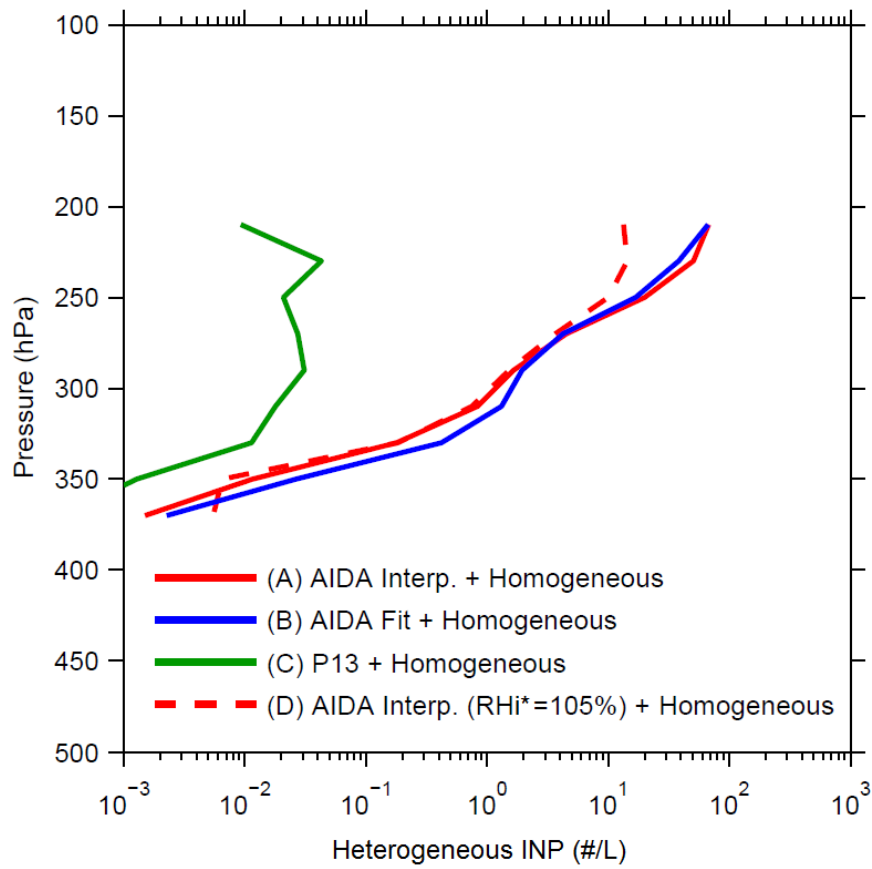
901

902

Figure 6.

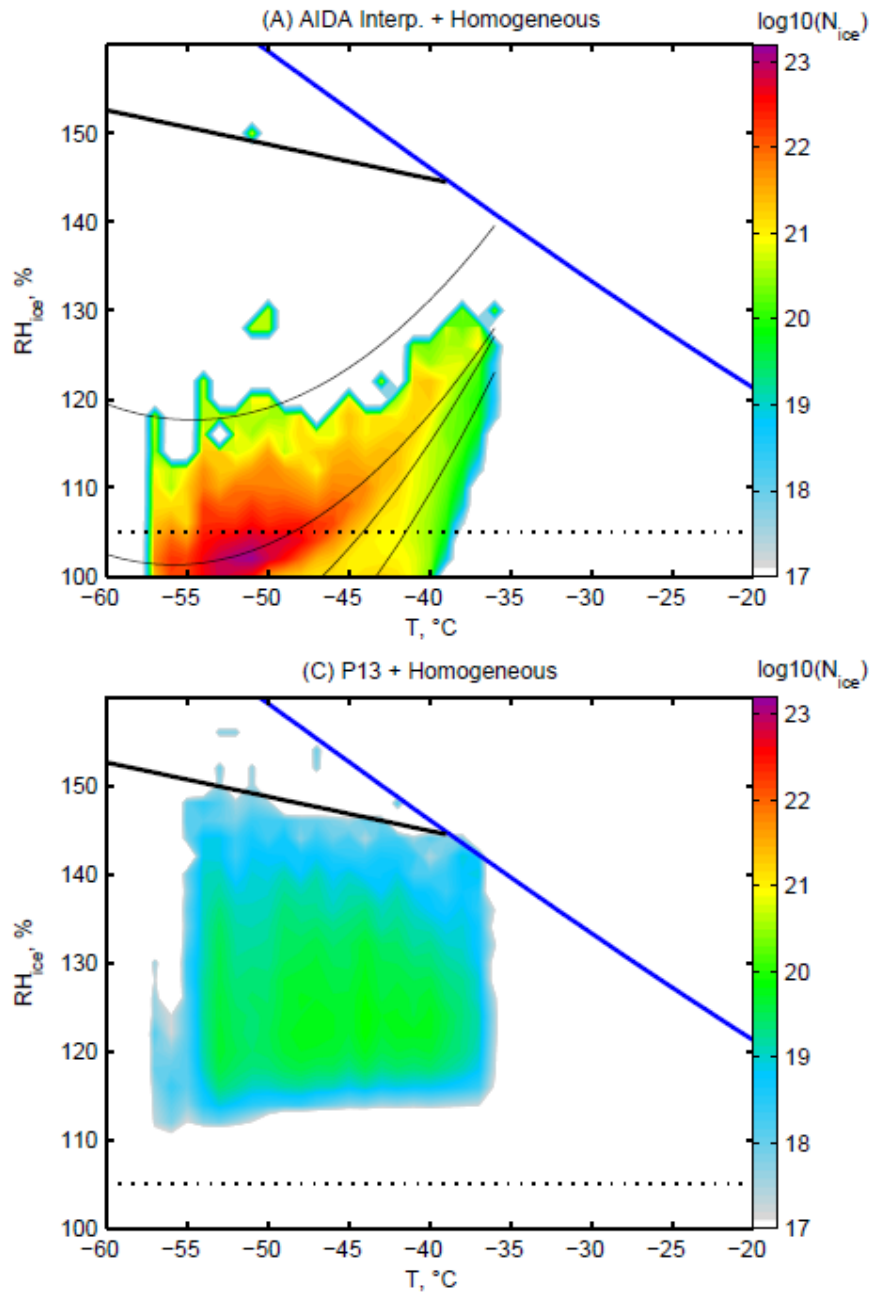


903



904  
905  
906

Figure 7.



907  
908

Figure 8.

## Figure Captions

Figure 1. Temporal plots of the representative AIDA deposition mode freezing experiments with various cooling ranges, including A. HALO06\_19, B. HALO06\_21, C. HALO05\_18 and D. HALO05\_24. Panels are arranged to show the measurements of i. AIDA mean gas temperature ( $T$ ), ii. TDL, iii. SIMONE and iv. ice crystal concentration ( $N_{ice}$ ). Note that the red lines represent interpolated data used for the  $n_s$ -isoline formulation. The  $I_{back,par}$  in Panel iv axis denotes the backscattered light scattering intensity parallel to the incident polarisation state (log-scaled). An increase in the depolarisation ratio indicates the formation and growth of ice crystals.

Figure 2. The constant  $n_s$  magnitudes are joined by lines (blue), representing “isolines” of hematite freezing profiles in the  $T$ - $RH_{ice}$  space. The interpolated isolines are equally spaced at every order of magnitude from  $10^{12} \text{ m}^{-2}$  (top) to  $10^9 \text{ m}^{-2}$  (bottom). Experimental trajectories of AIDA expansion-experiments with hematite particles are shown as red dotted lines. The data indicated by green color on the water saturation line represent the previously reported results of immersion freezing (Hiranuma *et al.*, 2014). The sub-panel shows a magnified section of  $T$  (-35 °C to -45 °C) and  $RH_{ice}$  (110 to 120 %) space with equi-distant  $n_s$  spacing (every quarter magnitude). The error bars at  $n_s$  of  $10^{12} \text{ m}^{-2}$  are from welas.

Figure 3. Ice nucleation onset  $T$ - $RH_{ice}$  of previously published data (A. AIDA studies, B. dust, and C. ammonium sulfate and organics) shown together with the isolines of hematite particles from the present study ( $10^{12} \text{ m}^{-2}$ , top, to  $10^9 \text{ m}^{-2}$ , bottom).

Figure 4. Spatial plot of isolines for constant  $n_s$  derived from A. interpolating AIDA data, B. applying the third degree polynomial fit function to interpolated AIDA data and C. a previously published parameterization (Phillips *et al.*, 2013) for hematite particles. The color scale displays log-scaled  $n_s$  values in  $\text{m}^{-2}$ , applicable to all panels. The solid black lines indicate the homogeneous freezing threshold line (i.e., Koop line).

Figure 5. Monthly mean profiles of the simulated in-cloud ice crystal number concentrations ( $N_i \sim N_{ice}$ ) over the ARM SGP site. The four cases shown in the figure include the pure

homogeneous ice nucleation case (HOM) and four combined (heterogeneous + homogeneous) ice nucleation cases: (A) AIDA Interp. + Homogeneous; (B) AIDA Fit + Homogeneous; (C) P13 + Homogeneous; and (D) AIDA Interp. ( $RH_i^* = 105\%$ ) + Homogeneous. Black dots show the observed mean profile of  $N_i$ . Left and right ends of the horizontal bars indicate the 10<sup>th</sup> and 90<sup>th</sup> percentiles of the observed  $N_i$  values at each pressure level.

Figure 6. Monthly mean profiles of the simulated in-cloud ice crystal number concentrations ( $N_i \sim N_{ice}$ ) over the ARM SGP site. The four cases shown in the figure include the pure homogeneous ice nucleation case (HOM) and four pure heterogeneous ice nucleation cases: (A) AIDA Interp.; (B) AIDA Fit; (C) P13; and (D) AIDA Interp. ( $RH_i^* = 105\%$ ). Black dots show the observed mean profile of  $N_i$ . Left and right ends of the horizontal bars indicate the 10<sup>th</sup> and 90<sup>th</sup> percentiles of the observed  $N_i$  values at each pressure level.

Figure 7. The mean heterogeneous INP number concentrations ( $\sim N_{ice}$ ) simulated in COSMO. The red dashed line represents the simulation with 105%  $RH_{ice}$  as the lower boundary of ice formation, while the others are based on with 100% for the minimum  $RH_{ice}$  value.

Figure 8. Accumulated ice crystal concentrations (color scale in total crystals per model domain) as a function of temperature (1°C bins) and  $RH_{ice}$  (2% bins). Heterogeneous nucleation simulated by AIDA parameterization (i.e., Figure 4A) and P13 parameterization (i.e., Figure 4C) was combined with homogeneous nucleation of cloud droplets.